A Joined Theoretical−Experimental Investigation on the ^{1}H and ^{13}C NMR Signatures of Defects in Poly(vinyl chloride)

Philippe d'Antuono, Edith Botek, and Benoît Champagne*

Laboratoire de Chimie Théorique Appliquée, Facultés Universitaires Notre-Dame de la Paix, rue de Bruxelles, 61, B-5000 Namur, Belgium

Joris Wieme, Marie-Françoise Reyniers, and Guy B. Marin

Laboratorium voor Chemische Technologie, Universiteit Gent, Krijgslaan 281 S5, B-9000 Gent, Belgium

Peter J. Adriaensens and Jan M. Gelan

Institute for Material Research, Chemistry Division, University of Hasselt, Universitaire Campus-Gebouw D, B-3590 Diepenbeek, Belgium

Received: June 27, 2008; Revised Manuscript Received: August 25, 2008

^{1}H and ^{13}C chemical shifts of PVC chains have been evaluated using quantum chemistry methods in order to evidence and interpret the NMR signatures of chains bearing unsaturated and branched defects. The geometrical structures of the stable conformers have been determined using molecular mechanics and the OPLS force field and then density functional theory with the B3LYP functional and the 6-311G(d) basis set. The nuclear shielding tensor has been calculated at the coupled-perturbed Kohn−Sham level (B3LYP exchange-correlation functional) using the 6-311+G(2d,p) basis set. The computational scheme accounts for the large number of stable conformers of the PVC chains, and average chemical shifts are evaluated using the Maxwell−Boltzmann distribution. Moreover, the chemical shifts are corrected for the inherent and rather systematic errors of the method of calculation by employing linear regression equations, which have been deduced from comparing experimental and theoretical results on small alkane model compounds containing Cl atoms and/or unsaturations. For each type of defect, PVC segments presenting different tacticities have been considered because it is known from linear PVC chains that the racemic (*meso*) dyads are characterized by larger (smaller) chemical shifts. NMR signatures of unsaturations in PVC chains have been highlighted for the internal −CH═CH− and −CH═CCl− units as well as for terminal unsaturations like the chloroallylic −CH═CH−CH_2Cl group. In particular, the ^{13}C chemical shifts of the two sp^2 C atoms are very close for the chloroallylic end group. The CH_2 and CHCl units surrounding an unsaturation present also specific ^{13}C chemical shifts, which allow distinguishing them from the others. In the case of the proton, the CH_2 unit of the −CHCl−CH_2−CCl═CH− segment presents a larger chemical shift (2.6−2.7 ppm), while some CHCl units close to the −CH═CH− unsaturations appear at rather small chemical shifts (3.7 ppm). The −CH_2Cl and −CHCl−CH_2Cl branches also display specific signatures, which result in large part from modifications of the equilibrium conformations and their reduced number owing to the increased steric interactions. These branches lead to the appearance of ^{13}C peaks at lower field associated either to the CH unit linking the −CH_2Cl and −CHCl−CH_2Cl branches (50 ppm) or to the CHCl unit of the ethyl branches (60 ppm). The corresponding protons resonate also at specific frequencies: 3.5−4.0 ppm for the −CH_2Cl branch or 3.8−4.2 ppm for the terminal unit of the −CHCl−CH_2Cl branch. Several of these signatures have been detected in the experimental ^{1}H and ^{13}C NMR spectra and are consistent with the reaction mechanisms.

I. Introduction

Poly(vinyl chloride) (PVC) is one of the important commodity polymers. It is prepared via a radical polymerization process, including the usual initiation, propagation, chain transfer, and termination steps. However, the real mechanism is far more complicated due to the occurrence of side reactions and due to the chain-length dependence of the kinetic parameters associated with the elementary reactions. Due to the occurrence of side reactions, structural irregularities are built into the polymer chains. PVC samples can be characterized by the concentrations and distributions of branches, of internal double bonds, and of the relative configurations of the stereogenic centers. Subsequently, these molecular (at the level of the unit cells) aspects determine the microstructure of PVC, the solid-state physical properties and morphologies of the resins, and also their chemical stability.[1]

The identification and the characterization of these defects have already been the focus of much research, a large part of it using high resolution NMR spectroscopy,[2] owing to the potential of NMR to unravel structural and electronic properties of molecules and polymers.[3] Moreover, a detailed knowledge of these concentrations and distributions can be used to elaborate kinetic models and then to master the experimental conditions in order to produce PVC with specific characteristics for targeted applications.[4] For instance, the presence of branch structures has been deduced from ^{13}C NMR spectra of PVC samples that

10.1021/jp805676q CCC: $40.75
Published on Web 11/01/2008

have been subjected to reductive dechlorination[2e,i] because of the difficulty of a direct NMR examination of PVC. Then, from the structural characterizations, the degree of chain and hydrogen transfer reactions was inferred. Nevertheless, the complexity of the relationship between the chemical shifts and the structures requires further investigations, in particular for interpreting the ^{1}H and ^{13}C NMR spectra and for assigning the NMR signatures to specific unsaturations and branches. Indeed, the heterogeneous suspension polymerization, employed at the industrial scale, leads to the formation, though in small concentrations, of structural defects such as tertiary chlorines at branched carbons, allylic chlorines, and oxygen-containing groups, each having a potential NMR signature. Nowadays, it is believed that the tertiary chlorines (with butyl and longer branches) and the allylic chlorines are the most abundant labile defects in PVC. The most abundant side chain structures are the chloromethyl branches (3.3−4.8/1000 VC), 2,4-dichlorobutyl branches (0.5−1.7/1000 VC), 1,2-dichloroethyl branches (0.1−0.6/1000 VC), and long chain branches (0.1−2.0/1000 VC).[2]

To address this issue, we have initiated a joined theoretical−experimental investigation aiming at interpreting the ^{1}H and ^{13}C NMR spectra of PVC oligomers. The first step has consisted of determining linear regression parameters for Cl-containing compounds, tackling the reliability of different quantum chemistry approaches and assessing the importance of relativistic, solvent, basis set, and electron correlation effects.[5] Then, in earlier reports, the chemical shifts of model linear chains have been rationalized in terms of the relative configurations of the stereogenic centers—leading to isotactic, syndiotactic, and atactic PVC fragments—as well as in terms of their corresponding conformations induced essentially by steric interactions.[6] Here, we analyzed the NMR signatures of PVC segments bearing unsaturations and branches and we interpreted spectra recorded for a PVC sample prepared at industrially relevant conditions. In particular, we considered two types of unsaturations, defined by the −CH═CH− and −CH═CCl− units, and the abundant $-CH_2Cl$ and $-CHCl-CH_2Cl$ branches. Note that the $-CHCl-CH_2Cl$ groups are not solely present in PVC chains as branches but also as end groups following from the chain transfer to monomer reaction. The reaction mechanism of their formation has been addressed in several papers.[7]

II. Experimental Aspects

II. A. Polymerization Procedure. Vinyl chloride monomer was polymerized by suspension polymerization at a polymerization temperature of 338 K with an initiator *tert*-butyl peroxyneodecanoate concentration of 0.0785 wt %, based on the monomer.[4] The polymerization was carried out in a 0.002 m^3 stainless steel reactor. The reaction vessel was filled at 298 K with 0.7 kg of distilled deionized water containing suspension stabilizers. Subsequently, oxygen was removed by flushing with nitrogen. After adding the initiator and 0.3 kg of the vinyl chloride monomer, the reactor was heated to a polymerization temperature of 338 K in 30 min. During the polymerization, the three-bladed stirrer was set at 700 rpm. The polymerization process was stopped by rapidly cooling the reactor down in 2−3 min to 298 K. After removing the residual monomer, filtrating, washing, and drying, the monomer conversion was measured gravimetrically. For the PVC sample presented in this study, the measured monomer conversion was 75.9%.

II. B. Analysis Procedure. ^{13}C NMR spectra were recorded at 52.5 °C on a Varian Inova 400 (9.4 T) spectrometer in a dedicated 10 mm carbon probe. The PVC sample was prepared with a concentration of 200 mg/mL THF-d_8 to which 20 mM $Cr(acac)_3$ (chromium(III)triacetylacetonate) was added as a relaxation agent. To eliminate NOE effects, the decoupler was only gated on during acquisition (Inverse Gated Decoupling). The spectral parameters used were the following: a spectral width of 22 kHz, a preparation delay of 4 s, a 90° pulse angle of 12 μs, an acquisition time of 0.7 s, and 250 000 accumulations. The chemical shift axis was calibrated by means of the THF-d_8 resonances at 67.2 and 25.1 ppm from tetramethylsilane (TMS).

^{1}H NMR spectra were recorded at 45 °C on the same spectrometer in a dedicated 5 mm probe. The sample was prepared with a concentration of 5 mg/mL THF-d_8. The spectral parameters used were the following: a spectral width of 5 kHz, a similar filter bandwidth, a 90° pulse angle of 5 μs, an acquisition time of 2.5 s, a preparation delay of 7.5 s, and 1000 accumulations. The chemical shift axis was calibrated by means of the THF-d_8 resonances at 3.57 and 1.72 ppm from TMS.

III. Theoretical and Computational Considerations

During the last decades, valuable tools to calculate and interpret NMR spectra of molecules and polymers have been elaborated. Some of these, applicable to small molecules, reach a very high accuracy on the chemical shifts by accounting for electron correlation, relativistic, solvent, ro-vibrational, and temperature effects.[8] For instance, the coupled-cluster CCSD, CCSD(T), and CCSDT treatments provide, for nuclear magnetic shielding tensors, the quantitative accuracy required for establishing absolute NMR scales for various nuclei as well as for calibrating less expensive theoretical approaches.[9] However, such highly correlated methods are still nowadays restricted to rather small compounds. On the other hand, DFT schemes offer a good compromise between computational cost and reliability and therefore present the potential to assist in assigning experimental spectra.[10] As a matter of illustration, DFT calculations helped in the configuration determination or confirmation of passifloricin A,[11a] sparteines,[11b] gloriosaols A and B,[11c] and menthol diastereoisomers[11d] as well as in reinterpreting ^{1}H NMR spectra of the *E* and *Z* isomers of alkyl phenyl ketone phenylhydrazones,[11e] reassigning the structure of hexacyclinol to a diepoxide,[12a] and predicting structure−property functions of alternating copolymers of ethylene imine and ethylene oxide.[12b] Indeed, the errors on the chemical shifts are often systematic in nature and they can be corrected by using a linear regression procedure.[5,6,13] For instance, Rablen et al.[13c] have shown that the latter procedure can attain a root-mean-square error on the so-predicted ^{1}H chemical shifts in comparison with solution experimental values as small as 0.15 ppm. The determination of linear regression parameters is therefore an important and prerequisite step toward applying DFT-based procedures for computing the NMR chemical shifts in view of addressing molecular and polymeric structures. This approach was already followed in a number of cases including chlorocoannulenes,[14a] C_{10}-chloroterpenes,[14b] as well as alanine, valine, and leucine residues in solid peptides and in solvated proteins.[14c]

A standard computational strategy was adopted here and is based on our earlier investigations.[5,6] The geometry optimizations were carried out using the hybrid B3LYP exchange-correlation (XC) functional[15] and the 6-311G(d) basis set[16] with a tight convergence threshold on the residual forces on the atoms of 1.5×10^{-5} Hartree/Bohr or Hartree/radian. A broad sampling of the potential energy surface was performed in two steps with the preliminary molecular mechanics step employing the OPLS force field[17] followed by the B3LYP/6-311G(d) step for those

SCHEME 1: Routes to the Formation of Structures Containing (a) −CH=CH− and (b) −CH=CHCl− Internal Double Bonds in Suspension Polymerization of Vinyl Chloride

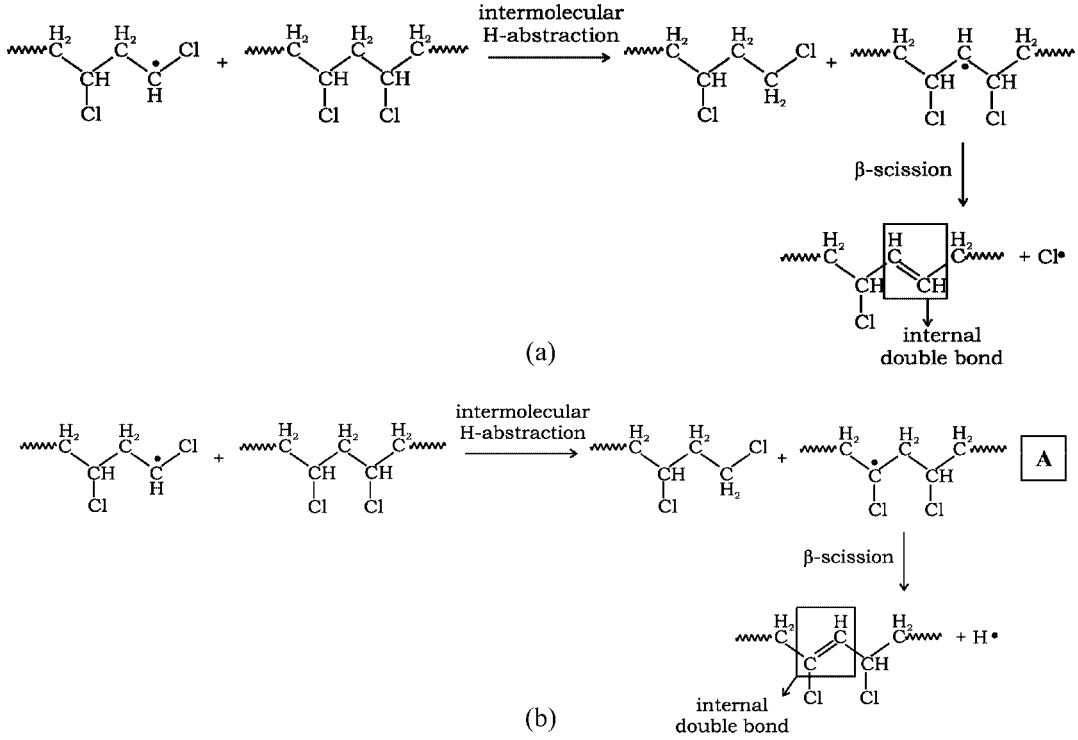

SCHEME 2: Route to Terminal Unsaturations in Free Radical Polymerization of Vinyl Chloride

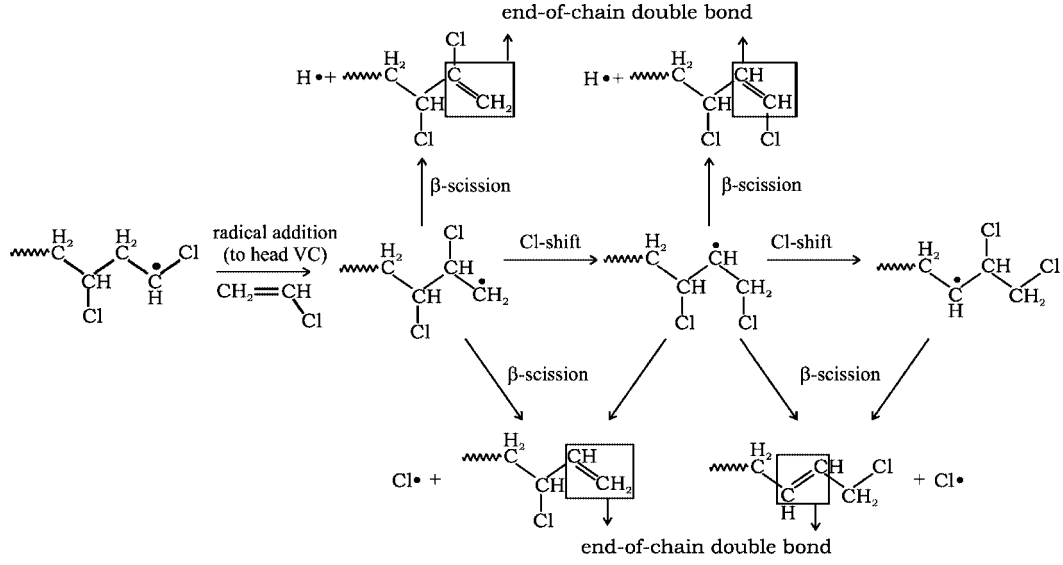

conformations of smaller energy (a threshold of 15 kJ/mol with respect to the global minimum was used). The NMR chemical shifts (δ_A, A = ^{1}H or ^{13}C) were calculated as the differences of isotropic shielding constants (σ) with respect to the tetramethylsilane (TMS) reference molecule. The σ value of TMS was determined at the same level of approximation (based on B3LYP/6-311G(d) optimized geometry) as for the different compounds, which enables part of the systematic errors to be reduced. The shielding tensor elements, corresponding to mixed second-order derivatives of the energy with respect to the external magnetic field, $\vec{B}$, and the magnetic moment of the nucleus, $\vec{m}_A$, were evaluated adopting the coupled-perturbed Kohn−Sham procedure[18] together with the gauge-invariant (or including) atomic orbital (GIAO) approach[19] to ensure origin independence of the shielding tensors. This method was employed at the B3LYP level of approximation with the 6-311+G(2d,p) basis set, which has been shown to be sufficient in several recent investigations of related compounds.[5,11e,13c]

When a molecule can adopt several stable conformations within a range of 15 kJ/mol, a Maxwell−Boltzmann (M-B) averaging of the conformers' chemical shifts is achieved. Following the study by Rablen et al.,[11e] the solvent effects were not accounted for directly in the simulation of the chemical shifts so that the linear regression coefficients derived from comparing experimental and theoretical data account not only for method limitations (electron correlation) but also for solvation. However, the impact of solvation effects on the Maxwell−Boltzmann distribution of conformers, and therefore on the chemical shifts, was also addressed. This was achieved within the polarizable continuum method using the integral equation formalism (IEF-

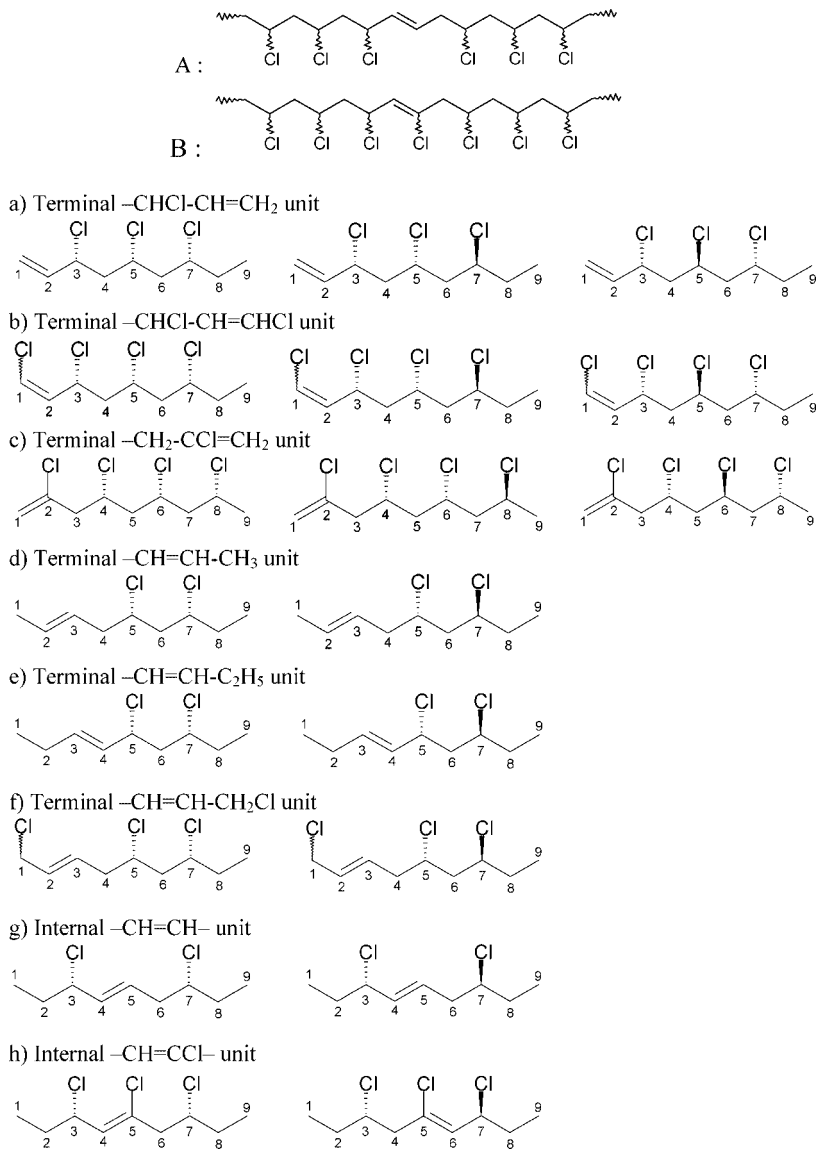

Figure 1. (top) Sketch of linear PVC fragments bearing the —CH═CH— (A) and —CH═CCl— (B) units. (bottom) Eight model (a—h) chains bearing unsaturation defects built from the 3,5,7-trichlorononane and the 2,4,6,8-tetrachlorononane and displaying different dyad/triad configurations. The backbone atom numbering is provided to help define the torsion angles and the chain conformations.

PCM) developed by Tomasi and co-workers.[20] All of the calculations were performed using the Gaussian 03 program.[21]

IV. Results and Discussion

This section is divided into three parts: (i) the determination and analysis of the geometrical structures of the chains bearing defects and the evaluation of the Maxwell—Boltzmann distribution of their stable conformers, (ii) the evaluation of their chemical shift signatures, and (iii) a discussion on the experimental data in the light of these simulations.

IV.A. Geometrical Structures. Chains incorporating unsaturations and branches were built from the 3,5,7-trichlorononane (triads) and 2,4,6,8-tetrachlorononane (tetrads) model compounds, respectively. These systems have previously been employed to investigate stereochemistry effects on the chemical shifts in linear chains of PVC.[6a]

IV.A.1. PVC Chains Bearing Unsaturations. During the PVC polymerization process, intermolecular H-abstraction and β-scission reactions can occur and lead to the formation of internal double bonds. A distinction can be made between two types of internal unsaturations, —CH═CH— and —CH═CCl—; see A and B of Figure 1. The —CH═CH— internal unsaturation is known to be the most frequently occurring internal unsaturation structure in PVC,[2h,22,23] and its mechanism of formation is illustrated in Scheme 1a. Little to no information is available on the occurrence and the mechanism of formation of the —CH═CCl— internal unsaturation. However, its presence in PVC chains cannot be excluded a *priori* and hence this structure is included in the present study. Scheme 1b illustrates a possible route leading to internal —CH═CCl— structures. The radical A, formed via the intermolecular H-abstraction reaction can, besides the β-scission reaction shown in Scheme 1b, also undergo other reactions such as, e.g., an addition reaction, resulting in the formation of a long chain branch carrying tertiary chlorine. The importance of the —CH═CCl— internal unsaturations in the resulting polymer molecules depends on their rate of formation relative to the rate of formation of the other defects. As the rate of the monomolecular β-scission reaction involved in the formation of internal —CH═CCl defect is not influenced by diffusion, their occurrence can become more important at high monomer conversion. Unsaturations can also be formed at terminal positions. A distinction can be made

between a number of terminal unsaturated structures; see structures **a**−**f** in Figure 1. The reaction mechanism leading to the formation of these terminal unsaturated structures is shown in Scheme 2 and involves a head-to-head addition reaction followed by Cl-shift reactions and a β-scission reaction. We therefore built from the 3,5,7-trichlorononane triad or 2,4,6,8-tetrachlorononane tetrad eight species containing successively terminal (**a**) −CHCl−CH=CH_2, (**b**) −CHCl−CH=CHCl, (**c**) −CH_2−CCl=CH_2, (**d**) −CH=CH−CH_3, (**e**) −CH=CH−CH_2−CH_3, and (**f**) −CH=CH−CH_2Cl units as well as internal (**g**) −CH=CH− and (**h**) −CH=CCl− units (Figure 1). The choice of structures **a**−**c** and **f**−**h** is obvious from the reaction mechanisms described in Schemes 1 and 2, whereas the study of defects **d** and **e** finds mostly a theoretical justification to create a reference point for the calculation of chemical shifts of structures containing either or both internal and terminal unsaturations. Compound **e** is also considered to assess solvent effects.

Like for the linear species, the relative configurations of the CHCl carbons define *meso* (*m*) and racemic (*r*) dyads, so that each unsaturation defect is associated with two or three isomers in order to model the chains. Moreover, these species are characterized by several stable conformations, which mostly differ by their backbone torsion angles. In the following, the conformers are described by their C2C3C4C5, C3C4C5C6, C4C5C6C7, and C5C6C7C8 torsion angles (θ), which are further associated with conformation labels. Those include the situations corresponding to *trans* (T, $\theta = 180.0°$), eclipsed positive (E, $\theta = 120.0°$), eclipsed negative (E′, $\theta = -120.0°$), gauche positive (G, $\theta = 60.0°$), gauche negative (G′, $\theta = -60.0°$), and *cis* (C, $\theta = 0.0°$).

(a) Terminal −CHCl−CH=CH_2 Unit. Three stereoisomers (*mm*, *mr*, and *rr*) have been considered for this compound bearing a terminal −CH=CH_2 unit. Considering the energy range of 15 kJ/mol, 10 conformers were found for the *mm* species (the most stable one is associated with a G′TG′T conformation, which means that, within our convention, the $\theta_{C2C3C4C5}$, $\theta_{C3C4C5C6}$, $\theta_{C4C5C6C7}$, and $\theta_{C5C6C7C8}$ torsion angles are close to −60, 180, −60, and 180°, respectively) while 4 were found for the *mr* and *rr* triads (Supporting Information Figure 1S). Considering their most stable conformer, the relative stability of the three stereoisomers is *rr*, *mr* (2.6 kJ/mol), and *mm* (7.9 kJ/mol). The presence of a terminal −CH=CH_2 unit modifies little the conformation of the regular linear chains.

(b) Terminal −CHCl−CH=CHCl Unit. This structure exhibits much similarities with compound **a**. In the case of the *mm* stereoisomer, there are 14 conformers with non-negligible weight within the MB distribution scheme (Supporting Information Figure 3S). The most stable one is G′TG′T like for the **a** system. For the *mr* triad, 7 conformers are obtained with G′TTT being the most stable, while, for the *rr* structure, there are 5 stable conformers and the all-*trans* form is the most stable. The relative stability of the three stereoisomers is *rr*, *mr* (0.7 kJ/mol), and *mm* (5.2 kJ/mol). Again, with respect to the regular PVC chains, the presence of the terminal unsaturation has little impact on the conformation.

(c) Terminal −CH_2−CHCl=CH_2 Unit. This terminal unit has a larger impact on the chain conformations than the two previous ones. Indeed, for compound **c**, there are 11, 6, and 5 stable conformers for triads *mm*, *mr*, and *rr*, with the most stable adopting a G′TGT, GTGT, and GTTT structure, respectively (Supporting Information Figure 5S). Nevertheless, the relative stability of the three stereoisomers still decreases from *rr* to *mr* (4.0 kJ/mol) and *mm* (16.0 kJ/mol).

(d) Terminal −CH=CH−CH_3 Unit. The unsaturation is located at carbons 2 and 3 (labeled as 2=3) and the relative configuration of the CHCl sites attributes to the structure a *meso* (2=3-*m*) or a racemic (2=3-*r*) configuration (Figure 1). Considering the energy range of 15 kJ/mol, 17 stable conformers were found for the *meso* species (the most stable one is EG′G′T) and 7 for the racemic one (the most stable one is E′GTT) (Supporting Information Figure 7S). The difference in energy between the most stable conformers of the two stereoisomers amounts to 4.8 kJ/mol in favor of the racemic compound. The presence of a double bond modifies the regular helical (*mm*) or zigzag (*rr*) structure of the linear chain by incorporating a 90° kink in the chain backbone as a result of the two G′ conformations (Supporting Information Table 4S and Figure 8S).

(e) Terminal −CH=CH−CH_2CH_3 Unit. The unsaturation is here located at carbons 3 and 4, giving rise to a terminal ethyl group as well as a *meso* or racemic PVC dyad (Figure 1). For the *meso* structure, there are 9 stable conformers. The most stable one displays a TEG′T backbone conformation (Supporting Information Figure 9S). There are 5 conformers for the other stereoisomer with TETT as the most stable (Supporting Information Figure 9S). The relative stability of the *meso*/racemic structures is 1.2 kJ/mol in favor of the racemic one. In the *meso* species, this defect is again associated with a 90° kink in the chain backbone (Supporting Information Table 5S and Figure 10S), whereas, for the racemic compound, conformational deviations from the all-*trans* form are reduced.

(f) Terminal −CH=CH−CH_2Cl Unit. This situation is similar to the **a** case at the exception of the substitution of the Me group by a CH_2Cl group. The presence of a Cl atom in the terminal position modifies the relative energy ordering of the conformers of the *meso* species but not of the racemic one (Supporting Information Figure 11S). Nevertheless, the preferential conformation of stereoisomer *m* still corresponds to a helix with a terminal 90° kink. In the case of the isotactic dyad, the most stable structure corresponds to the E′GTG conformer, whereas the syndiotactic dyad displays a most stable E′GTT conformer (Supporting Information Table 6S and Figure 12S). Again, the racemic isomer is more stable than the *meso* one (4.2 kJ/mol).

(g) Internal −CH=CH− Unit. The presence of an internal unsaturation divides the chain into two segments with their own conformation. Since these segments only contain one asymmetric C atom, the difference of stability of the *meso* and racemic stereoisomer is negligible (0.1 kJ/mol in favor of the racemic one) and the stability ordering of the conformers is *quasi* similar. The preferred conformation for the *meso* structure is E′TE′T, whereas, for the racemic one, 17 conformers are obtained, among which E′TET is the most stable (Supporting Information Figure 13S). The torsion angles of the carbon backbone and of the substituents for the two most stable conformers of each stereoisomer are listed in Supporting Information Table 4S, while the conformers are represented in Supporting Information Figure 14S. These two structures present similarities, the major difference being the $\theta_{C4-C5-C6-C7}$ torsion angle, which goes from −116.0° for the *meso* compound to +120.2° for the racemic one (Supporting Information Table 7S).

(h) Internal −CH=CCl− Unit. The most stable conformation for the isotactic dyad (Supporting Information Figure 15S) is E′TE′G, demonstrating that the preferential position of the two growing segments with respect to the double bond is *anti* (a *syn* configuration leads to an increase of energy by about 7 kJ/mol). For the other, racemic, stereoisomer (Supporting Information Figure 15S), the most stable structure is E′TE′T. The latter

SCHEME 3: Reaction Mechanism Leading to the Formation of (a) Chloromethyl and (b) 1,2-Dichloroethyl Branches

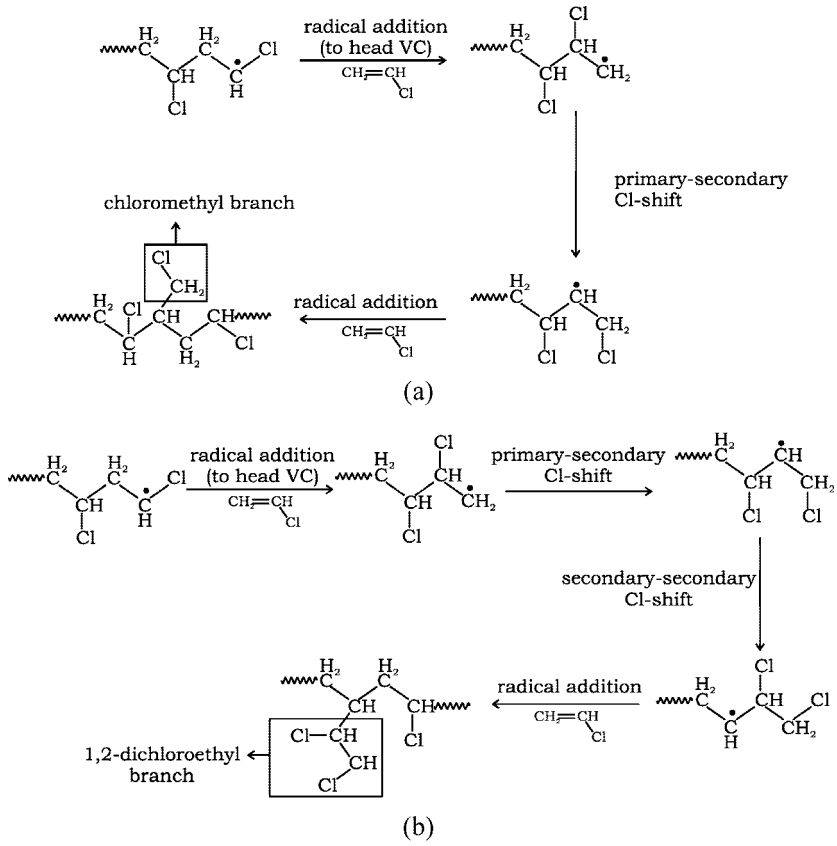

species is more stable by 1.4 kJ/mol, which means that with respect to an internal —CH=CH— unit the presence of a Cl atom on the double bond enhances the differentiation between the two stereoisomers (Supporting Information Table 8S and Figure 16S).

IV.A.2. PVC Chains Bearing Branches: —CH$_2$Cl and —CHCl—CH$_2$Cl. Frequently occurring structural defects in PVC are branches, and, in particular, the chloromethyl (—CH_2Cl) and 1,2-dichloroethyl (—CHCl—CH_2Cl) branches.[2c,k,21,22] Indeed, since they do not contain any tertiary chlorine or allyl chlorine, these structures are very stable. Their mechanism of formation, sketched in Scheme 3, involved the addition of a propagating macroradical to the head of a monomer molecule, followed by a primary−secondary chlorine shift, and by further additions of monomer to the formed radical. On the other hand, to form 1,2-dichloroethyl branches, the primary−secondary chlorine shift is followed by a secondary−secondary shift before the chain growing mechanism takes over.

Branched chains were built from the 2,4,6,8-tetrachlorononane chain by substituting the branches on the central CH_2 unit. A total of 10 stereoisomers was therefore considered. Indeed, starting from the *mmm*, *mrm*, *mmr*, *mrr*, *rmr*, and *rrr* tetrads, the addition of a branch at the C5 position leads to two possible configurations, except for the *mrm* and *rrr* cases where they are equivalent. These C5 configurations have been assigned to *cis* (*trans*) when the substituents on the C2 and C5 are on the same (opposite) side of the plane in the all-*trans* conformation (Figure 2). Adopting the same approach as for the linear chains and the chains bearing an unsaturation, the stable conformations were determined by B3LYP/6-311G(d) calculations and characterized by the torsion angles involving either the chain backbone ($\theta_{C1-C2-C3-C4}$, $\theta_{C2-C3-C4-C5}$, $\theta_{C3-C4-C5-C6}$, $\theta_{C4-C5-C6-C7}$, $\theta_{C5-C6-C7-C8}$, and $\theta_{C6-C7-C8-C9}$) or the branch ($\varphi_{C10-C5-C4-C6}$ and $\Psi_{Cl10-C10-C5-C4}$ for the —CH_2Cl and —CHCl—CH_2Cl groups and, in addition, $\gamma_{C11-C10-C5-C4}$ and $\delta_{Cl11-C11-C10-C5}$ for the —CHCl—CH_2Cl group).

(a) —CH$_2$Cl Branch. The structures of the most stable conformers of each stereoisomer are sketched in Supporting Information Figures 17S−22S, whereas the essential torsion angles are listed in Supporting Information Figure 23S. In most cases, the presence of the —CH_2Cl branch does not modify the conformation of the most stable conformer, with racemic dyads being associated to TT backbone conformations and *meso* dyads with TG or G′T conformations. For *mmm*, the most stable conformers are G′TG′TG′T and G′TG′TTG for the *cis* and *trans* cases (Supporting Information Figure 17S), the former being 8.3 kJ/mol more stable. For *mrm*, the G′TTTTG′ conformer presents the smallest energy, like its linear analog (Supporting Information Figure 18S). For both *cis* and *trans* branched cases of the *mmr* tetrad, the most stable conformer is G′TG′TTT, the *cis* one being more stable by 2.9 kJ/mol (Supporting Information Figure 19S). The preferred conformation for the *mrr-cis* and

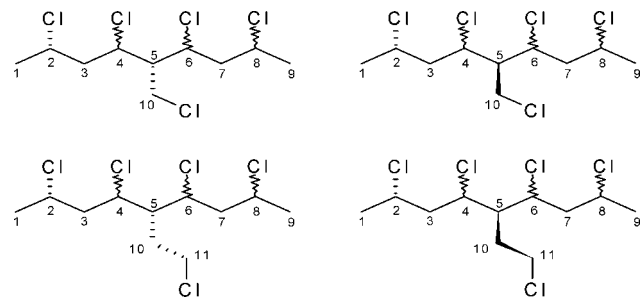

Figure 2. *cis* (left) and *trans* (right) configurations of the branches as illustrated for the —CH_2Cl (top) and —CHCl—CH_2Cl (bottom) branches as well as backbone atom numbering.

TABLE 1: Relative Stereoisomer Energies (kJ/mol) for Linear and Branched PVC Chains as Obtained at the B3LYP/6-311G(d) Level of Approximation from the Most Stable Conformer of 2,4,6,8-Tetrachloro-nonane and Its Analogs Bearing a $-CH_2Cl$ or $-CHCl-CH_2Cl$ Branch on the Central C Atom

			$-CH_2Cl$ branch		$-CHCl-CH_2Cl$ branch	
stereoisomers	most stable conformations	linear chains	*cis*	*trans*	*cis*	*trans*
rrr	TTTTTT	0.00	0.00	0.00	0.00	0.00
mrr	G′TTTTT	2.34	2.90	5.75	5.05	8.63
rmr	TTGTTT	3.97	3.36	−0.65	1.93	2.15
mmr	G′TG′TTT	5.70	3.48	6.42	4.09	7.33
mrm	G′TTTTG′	8.75	9.29	9.29	5.59	5.59
mmm	G′TG′TG′T	10.60	6.73	19.32	12.69	24.24

mrr-trans structures is G′TTTTT (Supporting Information Figure 20S), while the energy of the *cis* species is 2.8 kJ/mol lower. Then, for the *rmr* tetrad, placing a $-CH_2Cl$ branch at C5 leads to *cis* and *trans* structures exhibiting the same TTGTTT preferred conformation, with the Cl atom of the branch pointing as much outside as possible to reduce steric interactions (Supporting Information Figure 21S). Again, the *cis* species is more stable (4.3 kJ/mol). Finally, for the *rrr* stereoisomer, a TTTTTT conformation is found to be the most stable (Supporting Information Figure 22S).

(b) $-CHCl-CH_2Cl$ Branch. The important torsion angles are reported in Supporting Information Figure 24S, whereas the MB distributions are discussed elsewhere in the Supporting Information. Going from the small $-CH_2Cl$ branch to a twice longer branch reduces considerably, for any stereoisomer, the number of stable conformers in the [0, 12−15 kJ/mol] window, which is a direct consequence of the increased steric interactions and the restriction of favorable chain orientations. The *mmm* stereoisomer can adopt different stable conformations according to the position of the lateral group. Thus, for the *cis* position, the most stable structure is G′TG′TG′T, the other conformer having a much higher energy and not contributing to the MB distribution. In the *trans* position, the most stable conformer corresponds to G′TG′TE′T. For *mrm*, the most stable conformer is G′TTTTG′. TGTGTT is the most stable conformer for a *cis* position of the $-CHCl-CH_2Cl$ branch of the *mmr* stereoisomer, whereas for a *trans* positioning it is G′TG′TTT. Then, considering the *mrr* stereoisomer, the important conformers are TGTTTT (*cis*) and G′TTTTT (*trans*). The TTGTTT conformer is the most stable for both the *cis* and *trans rmr* stereoisomers. Finally, for the *rrr* situation, a TTTTTT conformer leads to the most stable structure.

Table 1 summarizes the relative stability of the different linear and branched stereoisomers. In the linear chain, the *rrr* tetrad is the most stable and adopts the TTTTTT conformation[6a] and the energy increases with the amount of *meso* dyads. For most of the stereoisomers of the branched chains, the most stable conformer corresponds to the most stable conformer of the linear chains, though, owing to modifications in the steric repulsions, the torsion angles are slightly different in the three cases. Among the situations with inversion, the *rmr-trans* stereoisomer is more stable than the *rrr* one in the case of a CH_2Cl substituent (0.65 kJ/mol), while, for the *cis* stereoisomer, $E_{rmr} > E_{rrr}$. Though other factors, including the kinetics of their formation, influence the relative population of the different tetrads, these relative stereoisomer energies are partly indicative of their statistical distributions. This statement is supported, for instance, by the ^{13}C NMR spectra of regular PVC where the *mmm* peak is much smaller than the *rrr* one.[24]

IV.B. Chemical Shifts. ***IV.B.1. Unsaturations.*** The ^{13}C and ^1H NMR chemical shifts were then calculated for the different stable conformers of the chains bearing an unsaturation. The values reported in Tables 2−9 account for the relative populations in the different conformers according to the Maxwell−Boltzmann distribution scheme. Moreover, they were corrected using linear regression equations previously obtained for the sp^2 C (eq 1),[6b] sp^3 C (eq 2),[5] H on sp^2 C (eq 3),[6b] and H on sp^3 C (eq 4):[5]

$$\delta(\text{Exp.}) = 0.6202\delta[\text{B3LYP/6-311+G(2d,p)}] + 41.87 \quad (1)$$

$$\delta(\text{Exp.}) = 0.7830\delta[\text{B3LYP/6-311+G(2d,p)}] + 2.50 \quad (2)$$

$$\delta(\text{Exp.}) = 0.8486\delta[\text{B3LYP/6-311+G(2d,p)}] + 0.64 \quad (3)$$

$$\delta(\text{Exp.}) = 0.9448\delta[\text{B3LYP/6-311+G(2d,p)}] + 0.08 \quad (4)$$

Note that similar conclusions could be drawn from using the linear regressions derived in ref 6b for the whole set of sp^2 and sp^3 C/H atoms. In the case of unsaturations, the ^{13}C and ^1H chemical shifts of the double bonds are specific and well-known, but theory can help in interpreting the effect of the surrounding atoms/groups. Similarly, the presence of double bonds modifies the chemical shifts of the surrounding groups, which constitute therefore indirect signatures of the presence of this type of defect.

First, the difference of ^{13}C chemical shifts between the two sp^2 C atoms of the unsaturated defects is an indicator of the type of unsaturation. Indeed, this difference is close to zero in the case of a terminal $-CH=CH-CH_2Cl$ unit ($\delta \sim 126$ ppm) and of a terminal $-CHCl-CH=CHCl$ unit ($\delta \sim 127$ ppm, except for the *rr* species), whereas it is close to 2 ppm (4−5 ppm) for a terminal $-CH=CH-CH_3$ ($-CH=CH-CH_2-CH_3$) unit. The difference is the largest for the terminal $-CHCl-CH=CH_2$ and $-CH_2-CCl=CH_2$ units with values of ∼14 and ∼22 ppm, respectively. Then, for an internal $-CH=CH-$ unit, the difference is also of the order of 4 ppm but the chemical shifts are 1−2 ppm smaller than in the case of a terminal $-CH=CH-CH_2-CH_3$ unit. An internal $-CH=CCl-$ unit displays a larger difference between the two chemical shifts (6 ppm corresponding to δ values of 128 and 134 ppm). In general, for the sp^2 C atoms, the chemical shifts slightly change when going from the racemic to the meso structures (Figure 1, Tables 2−9).

Next, we considered the sp^3 C atoms of the CHCl units surrounding the unsaturation. In the case of terminal defects, there is only one such unit, whereas, for internal defects, there are two. Besides defect **b** where they are smaller and defect **c** where they are similar, the chemical shifts are larger than in the corresponding regular PVC chains (56−58 ppm[6a]). For the **a** and **d**−**f** $-CH=CH-$ terminal defects, the ^{13}C chemical shifts of the CHCl units amount to 59−60 ppm for the *meso* species and to 60−61 ppm for the racemic ones. Therefore, these chemical shifts cannot help in distinguishing between these cases. On the other hand, the CHCl group adjacent to the $-CH=CHCl$ unsaturation in compound **b** presents a small δ value of ∼54 ppm. The CHCl units surrounding a $-CH=CCl-$

TABLE 2: ^{13}C and ^{1}H Chemical Shifts (ppm) for the Model PVC Chains Bearing a Terminal −CHCl−CH=CH$_2$ Defect (a of Figure 1) (The Values, Evaluated at the B3LYP/6-311+G(2d,p) Level of Approximation, Have Been Corrected Using eqs 1−4, while Considering the M-B Distribution for the Different Conformers at 383 K)

	mm	*mr*	*rr*
^{13}C			
$\underline{CH_2}$=CH−CHCl−CH$_2$−CHCl−CH$_2$−CHCl−CH$_2$−CH$_3$	117.64	117.74	116.94
CH$_2$=$\underline{CH}$−CHCl−CH$_2$−CHCl−CH$_2$−CHCl−CH$_2$−CH$_3$	131.14	131.21	132.06
CH$_2$=CH−$\underline{CHCl}$−CH$_2$−CHCl−CH$_2$−CHCl−CH$_2$−CH$_3$	58.99	58.55	59.52
CH$_2$=CH−CHCl−$\underline{CH_2}$−CHCl−CH$_2$−CHCl−CH$_2$−CH$_3$	43.15	44.90	44.40
CH$_2$=CH−CHCl−CH$_2$−$\underline{CHCl}$−CH$_2$−CHCl−CH$_2$−CH$_3$	58.04	58.67	59.07
CH$_2$=CH−CHCl−CH$_2$−CHCl−$\underline{CH_2}$−CHCl−CH$_2$−CH$_3$	42.82	44.42	44.86
CH$_2$=CH−CHCl−CH$_2$−CHCl−CH$_2$−$\underline{CHCl}$−CH$_2$−CH$_3$	61.84	62.04	61.85
^{1}H			
$\underline{CH_2}$=CH−CHCl−CH$_2$−CHCl−CH$_2$−CHCl−CH$_2$−CH$_3$	5.49	5.51	5.46
CH$_2$=$\underline{CH}$−CHCl−CH$_2$−CHCl−CH$_2$−CHCl−CH$_2$−CH$_3$	6.08	6.13	5.88
CH$_2$=CH−$\underline{CHCl}$−CH$_2$−CHCl−CH$_2$−CHCl−CH$_2$−CH$_3$	4.86	4.87	4.97
CH$_2$=CH−CHCl−$\underline{CH_2}$−CHCl−CH$_2$−CHCl−CH$_2$−CH$_3$	2.15	2.11	1.87
CH$_2$=CH−CHCl−CH$_2$−$\underline{CHCl}$−CH$_2$−CHCl−CH$_2$−CH$_3$	4.35	4.54	4.86
CH$_2$=CH−CHCl−CH$_2$−CHCl−$\underline{CH_2}$−CHCl−CH$_2$−CH$_3$	2.15	1.89	1.90
CH$_2$=CH−CHCl−CH$_2$−CHCl−CH$_2$−$\underline{CHCl}$−CH$_2$−CH$_3$	4.07	4.23	4.22

TABLE 3: ^{13}C and ^{1}H Chemical Shifts (ppm) for Model PVC Chains Bearing a Terminal −CHCl−CH=CHCl Defect (b of Figure 1) (The Values, Evaluated at the B3LYP/6-311+G(2d,p) Level of Approximation, Have Been Corrected Using eqs 1−4, while Considering the M-B Distribution for the Different Conformers at 383 K)

	mm	*mr*	*rr*
^{13}C			
$\underline{CHCl}$=CH−CHCl−CH$_2$−CHCl−CH$_2$−CHCl−CH$_2$−CH$_3$	126.26	127.19	125.65
CHCl=$\underline{CH}$−CHCl−CH$_2$−CHCl−CH$_2$−CHCl−CH$_2$−CH$_3$	126.82	127.58	128.28
CHCl=CH−$\underline{CHCl}$−CH$_2$−CHCl−CH$_2$−CHCl−CH$_2$−CH$_3$	53.29	53.48	54.63
CHCl=CH−CHCl−$\underline{CH_2}$−CHCl−CH$_2$−CHCl−CH$_2$−CH$_3$	41.59	43.44	43.37
CHCl=CH−CHCl−CH$_2$−$\underline{CHCl}$−CH$_2$−CHCl−CH$_2$−CH$_3$	56.74	57.88	57.99
CHCl=CH−CHCl−CH$_2$−CHCl−$\underline{CH_2}$−CHCl−CH$_2$−CH$_3$	42.64	44.56	44.93
CHCl=CH−CHCl−CH$_2$−CHCl−CH$_2$−$\underline{CHCl}$−CH$_2$−CH$_3$	61.25	62.13	61.86
^{1}H			
$\underline{CHCl}$=CH−CHCl−CH$_2$−CHCl−CH$_2$−CHCl−CH$_2$−CH$_3$	6.16	6.23	6.15
CHCl=$\underline{CH}$−CHCl−CH$_2$−CHCl−CH$_2$−CHCl−CH$_2$−CH$_3$	5.62	5.68	5.73
CHCl=CH−$\underline{CHCl}$−CH$_2$−CHCl−CH$_2$−CHCl−CH$_2$−CH$_3$	5.21	5.24	5.34
CHCl=CH−CHCl−$\underline{CH_2}$−CHCl−CH$_2$−CHCl−CH$_2$−CH$_3$	2.15	2.14	1.93
CHCl=CH−CHCl−CH$_2$−$\underline{CHCl}$−CH$_2$−CHCl−CH$_2$−CH$_3$	4.15	4.39	4.82
CHCl=CH−CHCl−CH$_2$−CHCl−$\underline{CH_2}$−CHCl−CH$_2$−CH$_3$	2.10	1.89	1.89
CHCl=CH−CHCl−CH$_2$−CHCl−CH$_2$−$\underline{CHCl}$−CH$_2$−CH$_3$	4.02	4.19	4.22

TABLE 4: ^{13}C and ^{1}H Chemical Shifts (ppm) for the Model PVC Chains Bearing a Terminal −CHCl−CH$_2$−CCl=CH$_2$ Defect (c of Figure 1) (The values, Evaluated at the B3LYP/6-311+G(2d,p) Level of Approximation, Have Been Corrected Using eqs 1−4, while Considering the M-B Distribution for the Different Conformers at 383 K)

	mm	*mr*	*rr*
^{13}C			
$\underline{CH_2}$=CCl−CH$_2$−CHCl−CH$_2$−CHCl−CH$_2$−CH$_2$−CH$_3$	117.32	116.45	116.15
CH$_2$=$\underline{CCl}$−CH$_2$−CHCl−CH$_2$−CHCl−CH$_2$−CH$_2$−CH$_3$	138.84	139.53	139.67
CH$_2$=CCl−$\underline{CH_2}$−CHCl−CH$_2$−CHCl−CH$_2$−CH$_2$−CH$_3$	42.63	44.80	44.41
CH$_2$=CCl−CH$_2$−$\underline{CHCl}$−CH$_2$−CHCl−CH$_2$−CH$_2$−CH$_3$	58.94	55.75	56.81
CH$_2$=CCl−CH$_2$−CHCl−$\underline{CH_2}$−CHCl−CH$_2$−CH$_2$−CH$_3$	41.41	41.08	41.33
CH$_2$=CCl−CH$_2$−CHCl−CH$_2$−$\underline{CHCl}$−CH$_2$−CH$_2$−CH$_3$	57.81	57.94	58.25
CH$_2$=CCl−CH$_2$−CHCl−CH$_2$−CHCl−$\underline{CH_2}$−CH$_2$−CH$_3$	42.96	43.00	45.04
^{1}H			
$\underline{CH_2}$=CCl−CH$_2$−CHCl−CH$_2$−CHCl−CH$_2$−CH$_2$−CH$_3$	5.34	5.23	5.22
CH$_2$=CCl−$\underline{CH_2}$−CHCl−CH$_2$−CHCl−CH$_2$−CH$_2$−CH$_3$	2.73	2.77	2.80
CH$_2$=CCl−CH$_2$−$\underline{CHCl}$−CH$_2$−CHCl−CH$_2$−CH$_2$−CH$_3$	4.26	4.34	4.70
CH$_2$=CCl−CH$_2$−CHCl−$\underline{CH_2}$−CHCl−CH$_2$−CH$_2$−CH$_3$	2.25	2.06	1.91
CH$_2$=CCl−CH$_2$−CHCl−CH$_2$−$\underline{CHCl}$−CH$_2$−CH$_2$−CH$_3$	4.17	4.73	4.74
CH$_2$=CCl−CH$_2$−CHCl−CH$_2$−CHCl−$\underline{CH_2}$−CH$_2$−CH$_3$	2.05	2.00	1.87

defect present similar characteristics to **d**−**f** (δ ∼60−61 ppm), whereas, for an internal −CH=CH− defect, the chemical shifts are larger and attain ∼64 ppm. Thus, if the C sp^2 signature is not sufficient to distinguish between defects **e** and **g**, the CHCl signature will help.

In the case of the CH_2 units surrounding the unsaturation, those associated with the terminal −CHCl−CH=CH$_2$, −CHCl−CH=CHCl, −CH$_2$−CCl=CH$_2$, and −CH=CH−CH$_3$ units as well as with the internal −CH=CH− units are similar, within 1 ppm, to those of the regular chains (δ = 40.5−43.2 ppm) so that, with the density of defects being small, the signatures of the defects will be hidden. On the other hand, the CH_2Cl of the −CH=CH−CH$_2$Cl terminal group possesses a larger chemical shift (∼46 ppm) so that it can be detected. A similar conclusion

TABLE 5: ^{13}C and ^{1}H Chemical Shifts (ppm) for the Model PVC Chains Bearing a Terminal $-CH=CH-CH_3$ Defect (d of Figure 1) (The Values, Evaluated at the B3LYP/6-311+G(2d,p) Level of Approximation, Have Been Corrected Using eqs 1−4, while Considering the M-B Distribution for the Different Conformers)

	meso	racemic
^{13}C		
$\underline{CH_3}-CH=CH-CH_2-CHCl-CH_2-CHCl-CH_2-CH_3$	18.78	18.70
$CH_3-\underline{CH}=CH-CH_2-CHCl-CH_2-CHCl-CH_2-CH_3$	127.32	127.17
$CH_3-CH=\underline{CH}-CH_2-CHCl-CH_2-CHCl-CH_2-CH_3$	125.15	125.62
$CH_3-CH=CH-\underline{CH_2}-CHCl-CH_2-CHCl-CH_2-CH_3$	38.49	40.31
$CH_3-CH=CH-CH_2-\underline{CHCl}-CH_2-CHCl-CH_2-CH_3$	60.49	60.37
$CH_3-CH=CH-CH_2-CHCl-\underline{CH_2}-CHCl-CH_2-CH_3$	42.92	43.90
$CH_3-CH=CH-CH_2-CHCl-CH_2-\underline{CHCl}-CH_2-CH_3$	62.38	62.72
^{1}H		
$\underline{CH_3}-CH=CH-CH_2-CHCl-CH_2-CHCl-CH_2-CH_3$	1.76	1.75
$CH_3-\underline{CH}=CH-CH_2-CHCl-CH_2-CHCl-CH_2-CH_3$	5.68	5.69
$CH_3-CH=\underline{CH}-CH_2-CHCl-CH_2-CHCl-CH_2-CH_3$	5.74	5.61
$CH_3-CH=CH-\underline{CH_2}-CHCl-CH_2-CHCl-CH_2-CH_3$	2.40	2.40
$CH_3-CH=CH-CH_2-\underline{CHCl}-CH_2-CHCl-CH_2-CH_3$	4.11	4.33
$CH_3-CH=CH-CH_2-CHCl-\underline{CH_2}-CHCl-CH_2-CH_3$	2.08	1.88
$CH_3-CH=CH-CH_2-CHCl-CH_2-\underline{CHCl}-CH_2-CH_3$	4.02	4.23

TABLE 6: ^{13}C and ^{1}H Chemical Shifts (ppm) for the Model PVC Chains Bearing a Terminal $-CH=CH-CH_2-CH_3$ Defect (e of Figure 1) (The Values, Evaluated at the B3LYP/6-311+G(2d,p) Level of Approximation, Have Been Corrected Using eqs 1−4, while Considering the M-B Distribution for the Different Conformers; the Values in Parentheses Have Been Obtained by Accounting for the Solvent Effects on the M-B Distribution within the IEFPCM Scheme)

	meso	racemic
^{13}C		
$CH_3-\underline{CH_2}-CH=CH-CHCl-CH_2-CHCl-CH_2-CH_3$	27.43 (27.41)	27.35 (27.29)
$CH_3-CH_2-\underline{CH}=CH-CHCl-CH_2-CHCl-CH_2-CH_3$	132.58 (133.92)	131.26 (132.60)
$CH_3-CH_2-CH=\underline{CH}-CHCl-CH_2-CHCl-CH_2-CH_3$	126.95 (126.71)	127.69 (127.43)
$CH_3-CH_2-CH=CH-\underline{CHCl}-CH_2-CHCl-CH_2-CH_3$	59.73 (61.36)	61.02 (62.66)
$CH_3-CH_2-CH=CH-CHCl-\underline{CH_2}-CHCl-CH_2-CH_3$	44.09 (43.94)	44.50 (46.30)
$CH_3-CH_2-CH=CH-CHCl-CH_2-\underline{CHCl}-CH_2-CH_3$	62.83 (64.37)	62.57 (64.20)
^{1}H		
$CH_3-\underline{CH_2}-CH=CH-CHCl-CH_2-CHCl-CH_2-CH_3$	2.10 (2.18)	2.08 (2.13)
$CH_3-CH_2-\underline{CH}=CH-CHCl-CH_2-CHCl-CH_2-CH_3$	5.81 (6.01)	5.76 (5.97)
$CH_3-CH_2-CH=\underline{CH}-CHCl-CH_2-CHCl-CH_2-CH_3$	5.47 (5.63)	5.61 (5.77)
$CH_3-CH_2-CH=CH-\underline{CHCl}-CH_2-CHCl-CH_2-CH_3$	4.66 (4.89)	4.82 (4.99)
$CH_3-CH_2-CH=CH-CHCl-\underline{CH_2}-CHCl-CH_2-CH_3$	2.13 (2.24)	1.97 (2.12)
$CH_3-CH_2-CH=CH-CHCl-CH_2-\underline{CHCl}-CH_2-CH_3$	3.81 (3.92)	4.24 (4.35)

TABLE 7: ^{13}C and ^{1}H Chemical Shifts (ppm) for Model PVC Chains Bearing a Terminal $-CH=CH-CH_2Cl$ Defect (f of Figure 1) (The Values, Evaluated at the B3LYP/6-311+G(2d,p) Level of Approximation, Have Been Corrected Using eqs 1−4, while Considering the M-B Distribution for the Different Conformers)

	meso	racemic
^{13}C		
$\underline{CH_2Cl}-CH=CH-CH_2-CHCl-CH_2-CHCl-CH_2-CH_3$	45.93	45.84
$CH_2Cl-\underline{CH}=CH-CH_2-CHCl-CH_2-CHCl-CH_2-CH_3$	126.18	126.07
$CH_2Cl-CH=\underline{CH}-CH_2-CHCl-CH_2-CHCl-CH_2-CH_3$	125.74	125.90
$CH_2Cl-CH=CH-\underline{CH_2}-CHCl-CH_2-CHCl-CH_2-CH_3$	38.76	39.82
$CH_2Cl-CH=CH-CH_2-\underline{CHCl}-CH_2-CHCl-CH_2-CH_3$	59.34	59.75
$CH_2Cl-CH=CH-CH_2-CHCl-\underline{CH_2}-CHCl-CH_2-CH_3$	43.29	44.12
$CH_2Cl-CH=CH-CH_2-CHCl-CH_2-\underline{CHCl}-CH_2-CH_3$	62.21	62.51
^{1}H		
$\underline{CH_2Cl}-CH=CH-CH_2-CHCl-CH_2-CHCl-CH_2-CH_3$	4.18	4.07
$CH_2Cl-\underline{CH}=CH-CH_2-CHCl-CH_2-CHCl-CH_2-CH_3$	5.72	5.71
$CH_2Cl-CH=\underline{CH}-CH_2-CHCl-CH_2-CHCl-CH_2-CH_3$	6.03	6.05
$CH_2Cl-CH=CH-\underline{CH_2}-CHCl-CH_2-CHCl-CH_2-CH_3$	2.49	2.48
$CH_2Cl-CH=CH-CH_2-\underline{CHCl}-CH_2-CHCl-CH_2-CH_3$	4.13	4.41
$CH_2Cl-CH=CH-CH_2-CHCl-\underline{CH_2}-CHCl-CH_2-CH_3$	2.12	1.88
$CH_2Cl-CH=CH-CH_2-CHCl-CH_2-\underline{CHCl}-CH_2-CH_3$	4.09	4.23

holds for the CH_2 group of the $-CH=CH-CH_2-CH_3$ terminal group with a chemical shift slightly higher than 27 ppm.

The ^{1}H chemical shifts for the H atoms attached to a sp^2 C atom also provide signatures of the presence of an unsaturation: they range from 5.2 to 6.2 ppm. The difference between the chemical shifts of the two protons can also help distinguishing between the **a**−**b** and **d**−**g** types of defects. Indeed, the difference is small (less than 0.1 ppm) for a terminal $-CH=CH-CH_3$ unit (**d** defect) and larger (0.2−0.3 ppm) for the **e** and **f** types of terminal unsaturations. Then, it gets even larger (0.4−0.6 ppm) for defects **a** and **b** where the unsaturation is located at the extremity of the chain. In the **a**, **b**, **e**, and **g**

TABLE 8: ^{13}C and ^{1}H Chemical Shifts (ppm) for the Model PVC Chains Bearing an Internal −CH═CH− Defect (g of Figure 1) (The Values, Evaluated at the B3LYP/6-311+G(2d,p) Level of Approximation, Have Been Corrected Using eqs 1−4, while Considering the M-B Distribution for the Different Conformers)

	meso	racemic
^{13}C		
$CH_3-\underline{CH_2}-CHCl-CH=CH-CH_2-CHCl-CH_2-CH_3$	31.33	31.43
$CH_3-CH_2-\underline{CHCl}-CH=CH-CH_2-CHCl-CH_2-CH_3$	64.20	64.52
$CH_3-CH_2-CHCl-\underline{CH}=CH-CH_2-CHCl-CH_2-CH_3$	130.79	130.88
$CH_3-CH_2-CHCl-CH=\underline{CH}-CH_2-CHCl-CH_2-CH_3$	126.43	126.35
$CH_3-CH_2-CHCl-CH=CH-\underline{CH_2}-CHCl-CH_2-CH_3$	39.90	39.80
$CH_3-CH_2-CHCl-CH=CH-CH_2-\underline{CHCl}-CH_2-CH_3$	64.47	64.74
^{1}H		
$CH_3-\underline{CH_2}-CHCl-CH=CH-CH_2-CHCl-CH_2-CH_3$	1.74	1.74
$CH_3-CH_2-\underline{CHCl}-CH=CH-CH_2-CHCl-CH_2-CH_3$	4.22	4.21
$CH_3-CH_2-CHCl-\underline{CH}=CH-CH_2-CHCl-CH_2-CH_3$	5.72	5.70
$CH_3-CH_2-CHCl-CH=\underline{CH}-CH_2-CHCl-CH_2-CH_3$	5.77	5.87
$CH_3-CH_2-CHCl-CH=CH-\underline{CH_2}-CHCl-CH_2-CH_3$	2.43	2.41
$CH_3-CH_2-CHCl-CH=CH-CH_2-\underline{CHCl}-CH_2-CH_3$	3.70	3.74

TABLE 9: ^{13}C and ^{1}H Chemical Shifts (ppm) for the Model PVC Chains Bearing an Internal −CH═CCl− Defect (h of Figure 1) (The Values, Evaluated at the B3LYP/6-311+G(2d,p) Level of Approximation, Have Been Corrected Using eqs 1 and 2, while Considering the M-B Distribution for the Different Conformers)

	meso	racemic
^{13}C		
$CH_3-\underline{CH_2}-CHCl-CH=CCl-CH_2-CHCl-CH_3-CH_2$	31.17	30.28
$CH_3-CH_2-\underline{CHCl}-CH=CCl-CH_2-CHCl-CH_3-CH_2$	60.28	60.52
$CH_3-CH_2-CHCl-\underline{CH}=CCl-CH_2-CHCl-CH_2-CH_3$	128.17	127.95
$CH_3-CH_2-CHCl-CH=\underline{CCl}-CH_2-CHCl-CH_2-CH_3$	134.30	134.04
$CH_3-CH_2-CHCl-CH=CCl-\underline{CH_2}-CHCl-CH_2-CH_3$	43.98	43.80
$CH_3-CH_2-CHCl-CH=CCl-CH_2-\underline{CHCl}-CH_2-CH_3$	61.69	61.75
^{1}H		
$CH_3-\underline{CH_2}-CHCl-CH=CCl-CH_2-CHCl-CH_2-CH_3$	1.72	1.73
$CH_3-CH_2-\underline{CHCl}-CH=CCl-CH_2-CHCl-CH_2-CH_3$	4.69	4.75
$CH_3-CH_2-CHCl-\underline{CH}=CCl-CH_2-CHCl-CH_2-CH_3$	5.69	5.66
$CH_3-CH_2-CHCl-CH=CCl-\underline{CH_2}-CHCl-CH_2-CH_3$	2.70	2.64
$CH_3-CH_2-CHCl-CH=CCl-CH_2-\underline{CHCl}-CH_2-CH_3$	4.12	4.15

cases, the amplitude of the δ difference depends on the *meso* or racemic nature of the dyads and triads.

The ^{1}H of the CHCl units have been shown to appear in the 4.24−4.59 ppm region, the larger shielding being associated with the *mm* triads. Calculations reproduce these effects, though the chemical shifts are overestimated by 0.2−0.3 ppm.[6a] Defect **a** presents CHCl δ values at the low field edge of the linear chain CHCl band with values between 4.86 and 4.97 ppm. On the other hand, defect **b** should be detectable because its δ value is larger and attains 5.2−5.3 ppm. For defect **c**, the δ values are smaller and similar to those of linear chains. In the case of the terminal −CH═CH−CH$_3$ and −CH═CH−CH$_2$Cl defects, the CHCl group is separated from the unsaturation by a methylene group and its ^{1}H chemical shift amounts to 4.1 ppm (4.3−4.4 ppm) for the *meso* (racemic) structures. Again, the larger shielding is a characteristic of the *meso* dyads. Peaks around 4.1 ppm are also found for the CHCl unit connected to an internal −CH═CCl− group by a methylene moiety (Table 9). Note that the internal −CH═CCl− defects also present chemical shifts at 4.7 ppm. Finally, in the internal −CH═CH− group, the most adjacent CHCl groups (one of these being attached to the unsaturation via a methylene segment) present chemical shifts of ∼4.2 and 3.7 ppm, the former one being in the region of the dominant CHCl band (and therefore it is predicted that it cannot be detected), whereas the latter being in the same region as the branch signatures (see the next section).

The CH$_2$ units of linear PVC chains present chemical shifts spanning the 1.8−2.2 ppm region as a function of the tacticity of the chain.[6a,23] δ values of similar amplitudes are calculated for chains with an unsaturation and, in particular, for those CH$_2$ units linked to a pair of CHCl groups (**a**, **b**, **d**, and **e**), the larger shieldings being associated with the racemic dyads. When the methylene group is attached to both a sp^2 C atom bearing a H atom and a CHCl group, the chemical shift attains 2.4−2.5 ppm. This can be the signature of the unsaturated defects **d**, **f**, or **g**. The chemical shift gets even larger (∼2.6−2.8 ppm) when the sp^2 C atom bears a Cl atom (defects **c** and **h**).

In summary, based on the ^{1}H chemical shift, one can distinguish between the different types of defects: (i) **a** and **b** present the largest differences of chemical shifts for the two protons attached to sp^2 C atoms, but the signal of the CHCl group adjacent to the unsaturation can only be detected for **b** because it is sufficiently large and attains 5.2−5.3 ppm; (ii) the internal −CH═CH− group (**g**) is characterized by a small δ value of 3.7 ppm for the CHCl group; (iii) for the internal −CH═CCl− group (**h**), the δ values of the CH$_2$ unit are as large as 2.6−2.7 ppm; (iv) it is even larger (2.7−2.8 ppm) for a terminal −CCl═CH$_2$ unit (**c**); (v) terminal −CH═CH−CH$_3$ (**d**) and −CH═CH−CH$_2$Cl (**e**) units possess a CH$_2$ signal around 2.4 ppm, but for the latter, the chemical shifts of the two H attached to the sp^2 C atom are much different.

The effects of the solvent (CHCl$_3$) on the chemical shifts were assessed by considering the change in Maxwell−Boltzmann distribution and therefore the modifications of the averaged chemical shifts. Since the least-squares fits have been carried out from experimental data of solvated species and calculated values obtained for gas phase species,[5,6] it is not appropriate to take into account the direct solvent effects, provided eqs 1−4

TABLE 10: Representative ^{13}C and ^{1}H Chemical Shifts (ppm) for a Model PVC Chain Bearing a CH_2Cl Branch in Comparison with the Linear PVC Chains (The Values, Evaluated at the B3LYP/6-311+G(2d,p) Level of Approximation, Have Been Corrected Using eqs 2 (^{13}C) and 4 (^{1}H) and Take into Account the M-B Distribution of the Different Conformers)

stereoisomers	central CH_2 group of the linear tetrad	CH branching site for the CH_2Cl branch (C5/H5)		CH_2Cl branch (C10/H10)	
		cis	*trans*	*cis*	*trans*
		^{13}C			
mmm	41.3	47.5	51.3	42.1	42.5
mmr	43.2	49.2	49.9	42.2	42.2
mrm	43.4	49.3	49.3	42.0	42.0
mrr	43.7	49.7	51.0	42.6	42.3
rmr	43.7	49.8	50.3	42.9	42.5
rrr	44.1	51.3	51.3	42.9	42.9
		^{1}H			
mmm	2.06	2.41	2.39	3.88	3.78
mmr	2.10	2.32	2.38	4.01	3.81
mrm	1.90	2.13	2.13	3.55	3.55
mrr	1.86	2.13	2.02	3.54	3.53
rmr	2.14	2.42	2.39	3.83	3.81
rrr	1.86	2.02	2.02	3.53	3.53

TABLE 11: Representative ^{13}C and ^{1}H Chemical Shifts (ppm) for a Model PVC Chain Bearing a $CHCl-CH_2Cl$ Branch in Comparison with the Linear PVC Chains (The Values, Evaluated at the B3LYP/6-311+G(2d,p) Level of Approximation, Have Been Corrected Using eqs 2 (^{13}C) and 4 (^{1}H) and Take into Account the M-B Distribution of the Different Conformers)

stereoisomers	central CH_2 group of the linear tetrad	CH branching site of the $CHClCH_2Cl$ unit (C_5/H_5)		CHCl unit of the $CHClCH_2Cl$ branch (C_{10}/H_{10})		CH_2Cl unit of the $CHClCH_2Cl$ branch (C_{11}/H_{11})	
		cis	*trans*	*cis*	*trans*	*cis*	*trans*
		^{13}C					
mmm	41.3	51.2	50.8	59.2	61.5	47.9	48.5
mmr	43.2	46.9	53.8	59.5	61.3	48.2	48.4
mrm	43.4	46.5	46.5	57.7	57.7	47.3	47.3
mrr	43.7	50.2	53.9	59.8	60.9	47.6	48.3
rmr	43.7	53.4	54.0	61.7	62.5	48.7	48.5
rrr	44.1	53.9	53.9	61.4	61.4	47.6	47.6
		^{1}H					
mmm	2.06	2.86	2.70	4.24	4.00	4.16	4.17
mmr	2.10	2.69	2.72	4.63	4.61	4.19	3.91
mrm	1.90	2.47	2.47	4.31	4.31	3.79	3.79
mrr	1.86	2.51	2.27	4.32	4.37	3.92	3.88
rmr	2.14	2.38	2.49	4.48	4.94	3.75	4.01
rrr	1.86	2.43	2.43	4.46	4.46	4.07	4.07

are employed. On the other hand, the indirect effects need to be considered because the set of reference compounds mostly include small molecules where generally 1−2 conformations are energetically favorable. As illustrated in Table 6 for the chain terminated by a $-CH=CH-C_2H_5$ segment, these variations of δ are systematic. In particular, the differences between the *meso* and racemic situations remain *quasi* unchanged.

IV.B.2. Branches: $-CH_2Cl$ and $-CHCl-CH_2Cl$. Table 10 lists the ^{13}C and ^{1}H chemical shifts representative of a $-CH_2Cl$ branch, *i.e.*, those of the CH group atoms to which the branch is attached as well as those of the C and H atoms of the branch itself (Figure 2). Table 11 provides the corresponding quantities for the $-CHCl-CH_2Cl$ branch. The chemical shifts were determined for the different stereoisomers at the B3LYP/6-311+G(2d,p) level of approximation and then corrected using linear relationships (eqs 2 and 4 for the ^{13}C and ^{1}H, respectively), while the usual Maxwell−Boltzmann distribution scheme is considered to obtain averaged values at 383 K (^{13}C) and 333 K (^{1}H). Adding a $-CH_2Cl$ branch to the central methylene unit modifies the ^{13}C δ values, since the C_5 atom goes from a secondary to a tertiary C atom. This is accompanied by an increase of the chemical shift of 7−11 ppm with respect to the linear PVC chains where they range between 41.3 and 44.1 ppm (as a function of the *m*/*r* content, the larger the *m* content, the smaller the chemical shift as a result of *gauche* interactions[3b]). This increase is not systematic: it depends on the type of tetrads and configurations. Note that, for the *cis* defects, δ increases with the number of racemic dyads, just like for the linear chains,[6a] but this trend is strongly modified for the *trans* structures. The presence of peaks in this region of the NMR spectrum, *i.e.*, on the left-hand side of the CH_2 peak, is expected to be visible and therefore to account for the presence of $-CH_2Cl$ branches. On the other hand, the presence of $-CH_2Cl$ branches could not be detected from the ^{13}C chemical shift of the branch itself because of the overlap between its peaks and those of the linear chains. Indeed, the associated chemical shifts, that do not change much between the *cis* and *trans* structures, range between 42.0 and 42.9 ppm.

Upon substitution, the spread of ^{1}H chemical shifts of the C_5 atom increases. In the regular chain, they range from 1.86 to 2.14 ppm, whereas, for the branched species, from 2.02 to 2.42 ppm. Therefore, depending upon the chain tacticity, these tertiary C signatures could overlap with those of CH_2 groups adjacent to unsaturations. The ^{1}H signatures of the $-CH_2Cl$ branch appear in the 3.53−4.01 ppm region, which therefore overlaps with the peaks of some of the CHCl units surrounding an unsaturation. Thus, the broad signal of the $^{1}H_{10}$ (see Figure 2 for the atom labeling, H_{10} is the H attached to the C_{10}) could

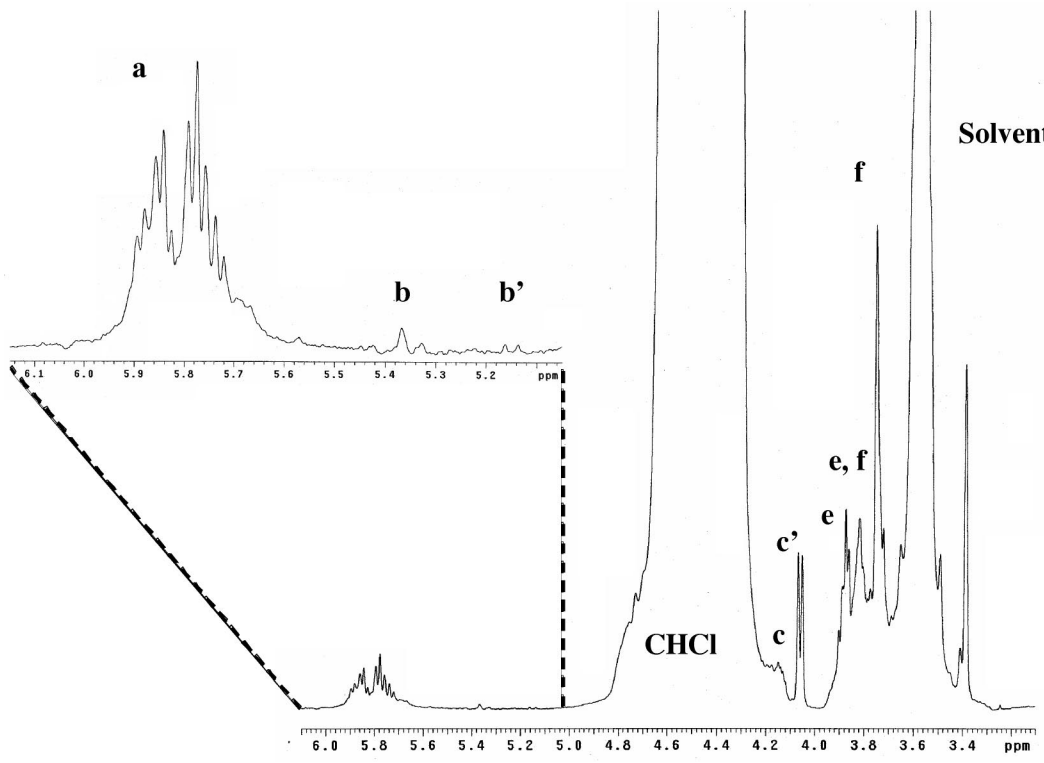

Figure 3. ^{1}H NMR spectrum of PVC.

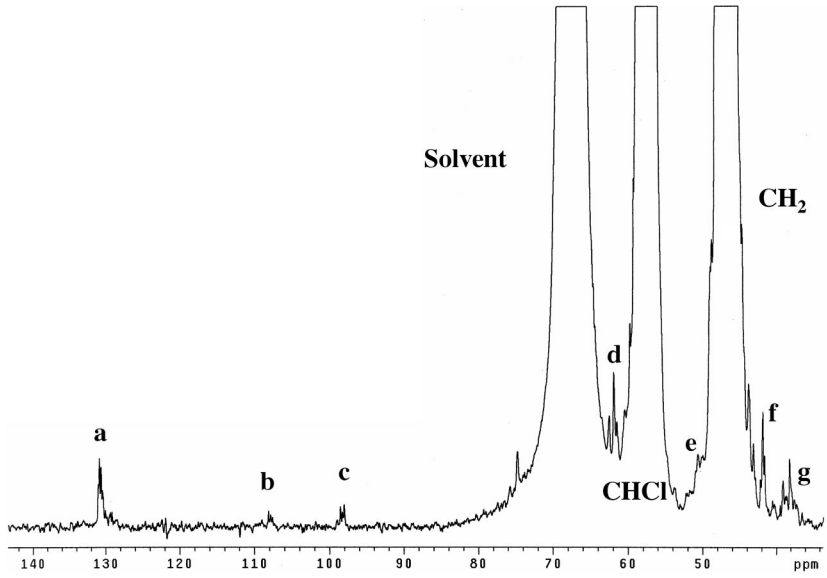

Figure 4. ^{13}C NMR spectrum of PVC.

mask the signature of the —CH═CH— internal units, but this signal will be distinguishable due to the many peaks associated with the different tetrads.

In the case of the —CHCl—CH_2Cl branch, the ^{13}C chemical shift of the tertiary C atom is further changed so that the smallest/largest δ value attains 46.5/54.0 ppm, demonstrating that the spread of the ^{13}C δ increases with the size of the branch. Moreover, the larger branch makes void this rule that associates a larger chemical shift to a tetrad with a larger racemic content. Going from a branch in the *cis* to *trans* position with respect to the chain backbone is often associated with an increase of δ (*mmr*, *mrr*, and, to a lower extent, *rmr*). For the parent *mmm* stereoisomer, the *cis* and *trans* positions lead to similar chemical shifts, which is consistent with the similarity between their most stable conformations (G′TG′TE′T and G′TG′TG′T). On the basis of their values, these signatures are expected to appear on the left side of the CH_2 regular chain peaks, overlapping therefore with those of the —CH_2Cl branch. The $^{13}C_{10}$ of the CHCl unit of the branch is deshielded by about 2−4 ppm with respect to the CHCl backbone signature occurring in the 56−58 ppm zone. Thus, this —CHCl—CH_2Cl branch signature appears in the same spectral zone as the CHCl units surrounding an unsaturation (**a**−**c** and **e** cases; see section IV.B.1). In addition, one observes a systematic increase of about 1 ppm from the *cis* to *trans* position of the branch. Finally, the terminal CH_2Cl unit presents a $^{13}C_{11}$ chemical shift close to 48 ppm, no matter which tetrad stereoisomer or branch position. In other words, one could say that the variations in $^{13}C_{11}$ δ are little affected by the config-

TABLE 12: Assignment of Experimental ^{1}H NMR Spectra of PVC Chains Bearing Defects by Using *ab initio* Calculations

experimental ^{1}H NMR	assignment ref 2k	analysis from *ab initio* calculations
a: 5.78−5.86 ppm	−CH=CH−CHCl− −CH=CH−CH_2Cl	−CH=CH−CHCl− [5.7−5.9 ppm] −CH=CH−CH_2Cl [5.7 ppm, but at 6.03 ppm, the other H is missing]
	−CHCl−CH=CH_2 −CHCl−CH=CHCl	−CHCl−CH=CH_2 [5.88−6.13 ppm] No −CHCl−CH=CHCl [6.15−6.23 ppm]
b: 5.34−5.38 ppm	−CHCl−CH=CHCl	−CHCl−CH=CH_2 [5.46−5.51 ppm]
b′: 5.14−5.17 ppm	−CH_2−CCl=CH_2 [or −CHCl−CH=CH_2 for both]	−CHCl−CH=CHCl [5.21−5.34 ppm] −CH_2−CCl=CH_2 [5.22−5.34 ppm]
c−c′: 4.14−4.06 ppm	*cis* and *trans* −CH=CH−CH_2Cl	−CH=CH−CH_2Cl [4.07−4.18 ppm] −CH=CH−CHCl− [4.21−4.22 ppm] −CH=CCl−CH_2−CHCl− [4.12−4.15 ppm]
d: 4.10 ppm	−CH_2−CH_2−O-CO-	−CHCl−CH_2−CH=CH−CH_2Cl [4.13−4.41]
e: 3.80−3.88 ppm	−CHCl−CH_2Cl	−CH_2Cl branch [3.7−3.8 ppm]
f: 3.74−3.80 ppm	−CH_2−CH_2Cl −CH_2Cl	−CHCl−CH_2Cl branch [3.8−4.0 ppm] −CH=CH−CH_2−CHCl− [3.70−3.74 ppm]

uration of the backbone. This value of 48 ppm is obviously close to other terminal CH_2Cl units, like those found in the unsaturation case **c** (46 ppm).

The ^{1}H chemical shift of H_5, on the anchoring C_5 atom, is further deshielded for the −CHCl−CH_2Cl branch with respect to the smaller −CH_2Cl branch. Indeed, the values range from 2.27 to 2.84 ppm, but it might be more relevant to point out that the parent *mmm* and *mmr* stereoisomers are characterized by δ values of about 2.7−2.8 ppm, whereas, for the other stereoisomers, the δ values are smaller. The ^{1}H signature of the CHCl segment of the branch appears in a broad region of the spectrum, from 4.00 to 4.94 ppm as a function of the chain configuration. This however occurs in the same region as the dominant CHCl backbone peaks so that it will hardly be detectable. The terminal branch CH_2Cl presents ^{1}H chemical shifts ranging from 3.75 to 4.19 ppm. It seems that the effect of the configuration is stronger for the ^{1}H than for the ^{13}C but they cannot be rationalized in terms of *meso* and racemic contents.

V. Further Comparison with Experimental Data and Discussion

In section IV, different types of defects have been characterized and their chemical shifts have been related to the chain configurations and conformations. It is now important to consider recorded spectra and to see how this theoretical information can help in assigning them. To do this, in addition to the results of section IV, we also take advantage of our previous works.[5,6] The ^{1}H and ^{13}C NMR spectrum of the PVC sample prepared and recorded according to section II are given in Figures 3 and 4, respectively. The ^{1}H NMR spectrum resembles for the largest part to the one reported by Purmova *et al.*,[2k] who discussed it in light of reaction mechanisms leading to the formation of different kinds of defects. Consequently, we decided to adopt the same labels as in ref 2k for the peaks. The main peaks, denoted a−f, are listed in Table 12 as well as their assignments.

Peaks a around 5.8 ppm has been associated to internal double bonds as well as to three types of terminal unsaturations. The *ab initio* calculations support the assignment to internal −CH=CH−, to terminal vinyl end, as well as to chloroallylic end groups, though, in the latter case, a second H(Csp^2) signal seems to be missing. On the other hand, the ^{1}H δ values of the defect **b** are too large (6.15−6.23 ppm) to match the 5.78−5.86 ppm signal and therefore to substantiate the presence of terminal −CHCl−CH=CHCl groups. This is further supported by the too large chemical shift of compound B [1,3-dichloro-1-propene] as presented in ref 6b.

The presence of terminal vinyl ends is supported by the ^{1}H signatures of the two H atoms attached to sp^2 C atoms. Indeed, in defect **a**, the calculations predict ^{1}H δ values of 5.88−6.13 ppm and of 5.46−5.51 ppm. The former matches the low field edge of the band spanning the 5.78−5.86 ppm region, whereas the latter agrees with signal b. Similar conclusions can be drawn from the results on the parent 3-chloro-1-butene compound,[6b] where the calculations predict ^{1}H δ values of 5.98 and 5.03−5.16 ppm, whereas the corresponding measured values amount to 6.00 and 5.07−5.23 ppm for protons similar to those of peaks a and b−b′, respectively. Signals b and b′ can also be attributed to the **a** and **c** defects.

Our calculations do not enable one to distinguish between peaks c−c′ and d, but they support the assignment of ref 2k. Moreover, other defects could be attributed to the peaks around 4.1 ppm including three types of CHCl units in close proximity to internal unsaturations.

Peaks e and f are assigned to the two types of branches (denoted methyl and ethyl branches) but not to the −CH_2−CH_2Cl branch. Indeed, calculations (as well as experimental data) on chloro-1-propane and chloro-1-butane predict smaller δ values for the latter case.[5] On the other hand, for the methyl and ethyl branches, our calculations support that both e and f peaks could be attributed to both types of branches, rather than specifically −CHCl−CH_2Cl to e and −CH_2Cl to f. Indeed, as seen in section IV.B.2, their chemical shifts span a rather large region owing to the different possible configurations of the chain backbone. The chloroallyl end group also displays a δ value around 3.7 ppm. A similar interpretation can be carried out based on the ^{1}H NMR spectrum of ref 2k, with the exception of the d peak at 4.10 ppm, which is attributed to the initiator end group.[25]

In addition to the linear backbone CH_2 and CHCl signals, the ^{13}C NMR spectra clearly evidence signals at 37−38−40 ppm (g), 42 ppm (f), 50 ppm (e), 62−63 ppm (d), and 130−131 ppm (a) next to smaller signals around 99 ppm (c) and 108 ppm (b). The peaks at 50 and 62−63 ppm can be attributed to the methyl and ethyl branches. However, the bands at 62−63 ppm could also find intensities from CHCl units nearby unsaturations (defects **g** and **h**). On the basis of the small separation between the peaks, the chloroallylic end (**f**) appears at 130−131 ppm. Note also the small upfield signal at 130 ppm

due to the *cis* form. Peaks at 37−42 ppm are associated with CH_2 groups close to unsaturations, whereas at high fields one can find these signals associated with chain ends. ^{13}C signals (mostly from sp^2 C) corresponding to the other defects detected on the ^{1}H spectra could not be found, probably because of too weak intensities.

VI. Conclusions

^{1}H and ^{13}C chemical shifts of PVC chains have been evaluated using quantum chemistry methods in order to evidence and interpret the NMR signatures of chains bearing unsaturated and branched defects. The computational procedure is based on a two-step geometry optimization employing molecular mechanics (OPLS force field) and then density functional theory (B3LYP/6-311G(d)) combined with nuclear shielding tensor calculations at the coupled-perturbed Kohn−Sham level (B3LYP exchange-correlation functional) using the 6-311+G(2d,p) basis set. This computational scheme accounts for the large number of stable conformers of the PVC chains, and average chemical shifts are evaluated using the Maxwell−Boltzmann distribution. Moreover, the chemical shifts are corrected for the inherent and rather systematic errors of the method of calculation by employing linear regression equations, which have been deduced from comparing experimental and theoretical results on small alkane model compounds containing Cl atoms and/or unsaturations. This approach was estimated to provide ^{1}H and ^{13}C chemical shifts within 0.1 and 1.0 ppm (4.0 ppm for sp^2 C atoms) of the experimental values.

NMR signatures of the presence of unsaturation in PVC chains have been highlighted for the internal −CH═CH− and −CH═CCl− units as well as for terminal unsaturations like the chloroallylic −CH═CH−CH_2Cl and vinyl −CHCl−CH═CH_2 groups. For each of these defects, PVC chains displaying different tacticities have been considered. Indeed, polymer chains are formed of successive racemic and/or *meso* dyads, which influence the chemical shifts: in linear chains, the racemic dyads characterizing syndiotactic polymers lead to preferential all-*trans* conformation and present larger chemical shifts, whereas smaller values are associated with isotactic chains, *meso* dyads, and *trans*−*gauche* conformations. In particular, the ^{13}C chemical shifts of the two sp^2 C atoms are very close for the chloroallylic end group, which provides a distinction with respect to the other unsaturations. In some cases, the CH_2 and CHCl units surrounding an unsaturation present a specific ^{13}C chemical shift, allowing to distinguish them from the others. In the case of the proton, the CH_2 unit of the −CHCl−CH_2−CCl═CH− segment presents a larger chemical shift (2.6−2.7 ppm), while some CHCl units close to the −CH═CH− unsaturations appear at rather small chemical shifts (3.7 ppm). Several of these signatures have been observed in the experimental spectra and well match the theoretical predictions. The so-called methyl (−CH_2Cl) and ethyl (−CHCl−CH_2Cl) branches also display specific signatures, which result in large part from modifications of the equilibrium conformations and their reduced number owing to the increased steric interactions. These branches lead to the appearance of ^{13}C peaks at lower field associated either to the CH unit linking the −CH_2Cl and CHCl−CH_2Cl branches (50 ppm) or to the CHCl unit of the ethyl branches (60 ppm). The corresponding protons resonate also at specific frequencies: 3.5−4.0 ppm for the −CH_2Cl branch or 3.8−4.2 ppm for the terminal unit of the −CHCl−CH_2Cl branch. Again, some of these signatures have been found in the experimental spectra, demonstrating the complementary contribution of theoretical modeling in the interpretation of NMR spectra of PVC chains bearing defects. Though comparison with experiment is still limited, the theoretical simulations have highlighted the rather strong sensitivity of the ^{1}H and ^{13}C chemical shifts on the tacticity of the chains bearing branches. Moreover, the tacticity effects in branched structures are clearly distinct from those of linear triads and tetrads where larger racemic content is associated with larger chemical shifts.

Acknowledgment. This work was supported from research grants from the Belgian Government (IUAP N° P5-03 "Supramolecular Chemistry and Supramolecular Catalysis" and IUAP N° P6-27 "Functional Supramolecular Systems"). Ph.d'A. is grateful to the F.R.I.A. ("Fonds pour la Formation à la Recherche dans l'Industrie et dans l'Agriculture) for financial support in the frame of his Ph.D. E.B. thanks the IUAP programs N° P5-03 and P6-27 for her postdoctoral grant. B.C. thanks the Fund for Scientific Research (FRS-FNRS) for his Research Director position. J.W. is a postdoctoral researcher of the Fund for Scientific Research-Flanders (F.W.O.-Vlaanderen). The calculations were performed thanks to the Interuniversity Scientific Computing Facility (ISCF), installed at the Facultés Universitaires Notre-Dame de la Paix (Namur, Belgium), for which the authors gratefully acknowledge the financial support of the FNRS-FRFC and the "Loterie Nationale" for the convention n° 2.4578.02, and of the FUNDP.

Supporting Information Available: Figures and tables with detailed information on the optimized geometrical structures of chains bearing unsaturated and branched defects. This material is available free of charge via the Internet at http://pubs.acs.org.

References and Notes

(1) Guyot, A. *Pure Appl. Chem.* **1985**, *57*, 833.

(2) (a) Hjertberg, T.; Sorvik, E. M. *Polymer* **1983**, *24*, 673. (b) Hjertberg, T.; Sorvik, E.; Wendel, A. *Makromol. Chem.* **1983**, *4*, 175. (c) Starnes, W. H., Jr.; Schilling, F. C.; Plitz, I. M.; Cais, R. E.; Freed, D. J.; Hartree, R. L.; Bovey, F. A. *Macromolecules* **1983**, *16*, 790. (d) Guyot, A. *Macromolecules* **1986**, *19*, 1090. (e) Starnes, W. H., Jr.; Wojciechowski, B. J.; Velasquez, A.; Benedikt, G. M. *Macromolecules* **1992**, *25*, 3638. (f) Rogestedt, M.; Hjertberg, T. *Macromolecules* **1993**, *26*, 60. (g) Xie, T. Y.; Hamielec, A. E.; Rogestedt, M.; Hjertberg, T. *Polymer* **1994**, *35*, 1526. (h) Starnes, W. H., Jr.; Chung, H.; Wojciechowski, B. J.; Skillicorn, D. E.; Benedikt, G. M. In *Polymer Durability*; *Advances in Chemistry Series*; 1996; Vol. 29. (i) Starnes, W. H., Jr.; Zaikov, V. G.; Chung, H. T.; Wojciechowski, B. J.; Tran, H. V.; Saylor, K. *Macromolecules* **1998**, *31*, 1508. (j) Starnes, W. H., Jr. *Prog. Polym. Sci.* **2002**, *27*, 2233. (k) Purmova, J.; Pauwels, K. F. D.; van Zoelen, W.; Vorenkamp, E. J.; Schouten, A. J.; Coote, M. L. *Macromolecules* **2005**, *38*, 6352.

(3) (a) Webb, G. A., Ando, I. In *Ann. Rept. NMR Spectroscopy*; Academic Press: London, 1997; Vol. 34 (Special Issue: NMR in Polymer Science). (b) Tonelli, A. E.; Schilling, F. C. *Acc. Chem. Res.* **1981**, *14*, 233.

(4) (a) De Roo, T.; Wieme, J.; Heynderickx, G. J.; Marin, G. B. *Polymer* **2005**, *46*, 8340. (b) Wieme, J.; De Roo, T.; Marin, G. B.; Heynderickx, G. J. *Ind. Eng. Chem. Res.* **2007**, *46*, 1179.

(5) d'Antuono, Ph.; Botek, E.; Champagne, B.; Spassova, M.; Denkova, P. *J. Chem. Phys.* **2006**, *125*, 144309.

(6) (a) d'Antuono, Ph.; Botek, E.; Champagne, B.; Wieme, J.; Reyniers, M.-F.; Marin, G. B.; Adriaensens, P. J.; Gelan, J. M. *Chem. Phys. Lett.* **2005**, *411*, 207. (b) d'Antuono, Ph.; Botek, E.; Champagne, B.; Wieme, J.; Reyniers, M.-F.; Marin, G. B.; Adriaensens, P. J.; Gelan, J. M. *Chem. Phys. Lett.* **2007**, *436*, 388.

(7) (a) Van Cauter, K.; Van Speybroeck, V.; Waroquier, M. *ChemPhysChem* **2007**, *8*, 541. (b) Van Cauter, K.; Van Den Bossche, B. J.; Van Speybroeck, V.; Waroquier, M. *Macromolecules* **2007**, *40*, 1321.

(8) (a) Helgaker, T.; Jaszunski, M.; Ruud, K. *Chem. Rev.* **1999**, *99*, 293. (b) Ando, I.; Kuroki, S.; Kurosu, H.; Yamanobe, T. *Prog. NMR Spectrosc.* **2001**, *39*, 79. (c) Gauss, J.; Stanton, J. F. *Adv. Chem. Phys.* **2002**, *123*, 355. (d) Kaupp, M., Bühl, M.; Malkin, V. G. *Calculation of NMR and EPR Parameters*; Wiley-VCH: Weinheim, Germany, 2004. (e) Bagno, A.; Rastrelli, F.; Saielli, G. *Chem.−Eur. J.* **2006**, *12*, 5514. (f) Bifulco, G.;

Dambruoso, P.; Gomez-Paloma, L.; Riccio, R. *Chem. Rev.* **2007**, *107*, 3744. (g) Casabianca, L. B.; de Dios, A. C. *J. Chem. Phys.* **2008**, *128*, 052201.

(9) (a) Gauss, J.; Stanton, J. F. *J. Chem. Phys.* **1995**, *102*, 251. (b) Gauss, J.; Stanton, J. F. *J. Chem. Phys.* **1996**, *104*, 2574. (c) Gauss, J. *J. Chem. Phys.* **2002**, *116*, 4773. (d) Auer, A. A.; Gauss, J.; Stanton, J. F. *J. Chem. Phys.* **2003**, *118*, 10407.

(10) (a) Malkin, V. G.; Malkina, O. L.; Casida, M. E.; Salahub, D. R. *J. Am. Chem. Soc.* **1994**, *116*, 5898. (b) Rauhut, G.; Puyear, S.; Wolinski, K.; Pulay, P. *J. Phys. Chem.* **1996**, *100*, 6310. (c) Olsson, L.; Cremer, D. *J. Chem. Phys.* **1996**, *105*, 8995. (d) Baldridge, K. K.; Siegel, J. S. *J. Phys. Chem. A* **1999**, *103*, 4038. (e) Cammi, R.; Mennucci, B.; Tomasi, J. *J. Chem. Phys.* **1999**, *110*, 7627. (f) Barone, G.; Gomez-Paloma, L.; Duca, D.; Silvestri, A.; Riccio, R.; Bifulco, G. *Chem.—Eur. J.* **2002**, *8*, 3233. (g) Poater, J.; van Lenthe, E.; Baerends, E. J. *J. Chem. Phys.* **2003**, *118*, 8584. (h) Keal, T. W.; Tozer, D. J. *J. Chem. Phys.* **2003**, *119*, 3015. (i) Allen, M. J.; Keal, T. W.; Tozer, D. J. *Chem. Phys. Lett.* **2003**, *380*, 70. (j) Bagno, A.; Rastrelli, F.; Saielli, G. *J. Phys. Chem. A* **2003**, *107*, 9964. (k) Tähtinen, P.; Bagno, A.; Klika, K. D.; Pihlaja, K. *J. Am. Chem. Soc.* **2003**, *125*, 4609. (l) Hieringer, W.; Della Sala, F.; Görling, A. *Chem. Phys. Lett.* **2004**, *383*, 115. (m) Arbuznikov, A. V.; Kaupp, M. *Chem. Phys. Lett.* **2004**, *386*, 8. (n) Wiitala, K. W.; Hoye, T. R.; Cramer, C. J. *J. Chem. Theory Comput.* **2006**, *2*, 1085. (o) Bagno, A.; Rastrelli, F.; Saielli, G. *J. Org. Chem.* **2007**, *72*, 7373. (p) Pennanen, T. S.; Lantto, P.; Sillanpää, A. J.; Vaara, J. *J. Phys. Chem. A* **2007**, *111*, 182.

(11) (a) Bifulco, G.; Gomez-Paloma, L.; Riccio, R. *Tetrahedron Lett.* **2003**, *44*, 7137. (b) Galasso, V.; Asaro, F.; Berti, F.; Przybyl, A. K.; Wlodarczak, J.; Wysocka, W.; Habus, I.; Kovac, B. *Chem. Phys.* **2005**, *314*, 25. (c) Bassarello, C.; Bifulco, G.; Montoro, P.; Skhirtladze, A.; Kemertelidze, E.; Pizza, C.; Piacente, S. *Tetrahedron* **2007**, *63*, 148. (d) Härtner, J.; Reinscheid, U. M. *J. Mol. Struct.* **2008**, *872*, 145. (e) Trabelsi, M.; Salem, M.; Champagne, B. *Org. Biomol. Chem.* **2003**, *1*, 3839.

(12) (a) Rychnovsky, S. D. *Org. Lett.* **2006**, *8*, 2895. (b) Sasanuma, Y.; Kumagai, R.; Nakata, K. *Macromolecules* **2006**, *39*, 6752.

(13) (a) Chesnut, D. B. *The ab initio Computation of Nuclear Magnetic Resonance Chemical Shielding*; VCH: Weinheim, Germany, 1996; Vol. 8. (b) Alkorta, I.; Elguero, J. *Struct. Chem.* **1998**, *9*, 187. (c) Rablen, P. R.; Pearlman, S. A.; Finkbiner, J. *J. Phys. Chem. A* **1999**, *103*, 7357. (d) Tanuma, T.; Irisawa, J.; Ohnishi, K. *J. Fluorine Chem.* **2000**, *102*, 205. (e) Chesnut, D. B. *Chem. Phys. Lett.* **2003**, *380*, 251. (f) Gryffer-Keller, A.; Molchanov, S. *Mol. Phys.* **2004**, *102*, 1903.

(14) (a) Baldridge, K. K.; Siegel, J. S. *Theor. Chem. Acc.* **2008**, *120*, 95. (b) Tuppurainen, K.; Ruuskanen, J. *Chemosphere* **2003**, *50*, 603. (c) Havlin, R. H.; Laws, D. D.; Bitter, H. M. L.; Sanders, L. K.; Sun, H.; Grimley, J. S.; Wemmer, D. E.; Pines, A.; Oldfield, E. *J. Am. Chem. Soc.* **2001**, *123*, 10362.

(15) (a) Becke, A. D. *J. Chem. Phys.* **1993**, *98*, 5648. (b) Lee, C.; Yang, W.; Parr, R. G. *Phys. Rev. B* **1988**, *37*, 785.

(16) (a) McLean, A. D.; Chandler, G. S. *J. Chem. Phys.* **1980**, *72*, 5639. (b) Krishnan, R.; Binkley, J. S.; Seeger, R.; Pople, J. A. *J. Chem. Phys.* **1980**, *72*, 650.

(17) (a) Jørgensen, W. L.; Tirado-Rives, J. *J. Am. Chem. Soc.* **1988**, *110*, 1657. (b) Pranata, J.; Wierschke, S.; Jørgensen, W. L. *J. Am. Chem. Soc.* **1991**, *113*, 2810. (c) Jørgensen, W. L.; Maxwell, D. S.; Tirado-Rives, J. *J. Am. Chem. Soc.* **1996**, *118*, 11225. (d) Rizzo, R. C.; Jørgensen, W. L. *J. Am. Chem. Soc.* **1999**, *121*, 4827.

(18) Cheeseman, J. R.; Trucks, G. W.; Keith, T. A.; Frisch, M. J. *J. Chem. Phys.* **1996**, *104*, 5497.

(19) (a) Ditchfield, R. *J. Am. Chem. Soc.* **1971**, *93*, 5287. (b) Wolinski, K.; Hilton, J. F.; Pulay, P. *J. Am. Chem. Soc.* **1990**, *112*, 8251.

(20) (a) Cancès, E.; Mennucci, B.; Tomasi, J. *J. Chem. Phys.* **1997**, *107*, 3032. (b) Tomasi, J.; Cammi, R.; Mennucci, B.; Cappelli, C.; Corni, S. *Phys. Chem. Chem. Phys.* **2002**, *4*, 5697.

(21) Frisch, M. J.; et al. *Gaussian 03*, revision B.04; Gaussian, Inc.: Pittsburgh, PA, 2003.

(22) (a) Starnes, W. H., Jr.; Shilling, F. C.; Abbas, K. B.; Cais, R. E.; Bovey, F. A. *Macromolecules* **1979**, *12*, 556. (b) Starnes, W. H. *J. Polym. Sci.* **2005**, *43*, 2451.

(23) Wieme, J.; Reyniers, M.-F.; Marin, G. B. *Chem. Eng. Sci.* **2007**, *62*, 5300.

(24) (a) Heatley, F.; Bovey, F. A. *Macromolecules* **1969**, *2*, 241. (b) Mirau, P. A.; Bovey, F. A. *Macromolecules* **1986**, *19*, 210.

(25) Ph. d'Antuono, unpublished results. Similar calculations were performed on *t*-But—CO—O—$C\underline{H}_2$—CHCl—CH_2—CHCl—CH_3 and have shown that the proton signal appears around 4.2−4.3 ppm in agreement with peak d of ref 2k.

JP805676Q